June 2017

Analytical Study Based Optimal Placement of Energy Storage Devices in Distribution Systems to Support Voltage and Angle Stability

Yih Der Kuo
University of Wisconsin-Milwaukee

ANALYTICAL STUDY BASED OPTIMAL PLACEMENT OF ENERGY STORAGE DEVICES IN DISTRIBUTION SYSTEMS TO SUPPORT VOLTAGE AND ANGLE STABILITY

by

Yih Der Kuo

A Thesis Submitted in

Partial Fulfillment of the

Requirements for the Degree of

Master of Science

in Engineering

at

The University of Wisconsin-Milwaukee

August 2017

ABSTRACT

ANALYTICAL STUDY BASED OPTIMAL PLACEMENT OF ENERGY STORAGE DEVICES IN DISTRIBUTION SYSTEMS TO SUPPORT VOLTAGE AND ANGLE STABILITY

by

Yih Der Kuo

The University of Wisconsin-Milwaukee, 2017
Under the Supervision of Professor Adel Nasiri

Larger penetration of Distributed Generations (DG) in the power system brings new flexibility and opportunity as well as new challenges due to the generally intermittent nature of DG. When these DG are installed in the medium voltage distribution systems as components of smart grid, further support is required to ensure smooth and controllable operation. To complement the uncontrollable output power of these resources, energy storage devices need to be incorporated to absorb excessive power and provide power shortage in time of need. They also can provide reactive power to dynamically help the voltage profile. Energy Storage Systems (ESS) can be expensive and only a limited number of them can

practically be installed in distribution systems. In addition to frequency regulation and energy time shifting, ESS can support voltage and angle stability in power network. This thesis applies a Jacobian matrix-based sensitivity analysis to determine the most appropriate node in a grid to collectively improve the voltage magnitude and angle of all the nodes by active/reactive power injection. IEEE 14-bus distribution system is selected to demonstrate the performance of the proposed method due to its clear and simple configuration. The developed technique is also applied to the IEEE 123-bus system to further evaluate the effectiveness and demonstrate the performance for a more complicated system. As opposed to most previous studies, this method does not require an iterative loop with convergence problem nor a network-related complicated objective function.

TABLE OF CONTENTS

LIST OF FIGURES

LIST OF TABLES

CHAPTER 1 OVERVIEW

Power systems nowadays are facing many problems, rising cost of fuel, emissions that causes climate change, stability issues and others. With availability, cost and environmental concerns of fossil fuel recognized, the need for new power sources is imminent. Distribution power sources are growing gradually to provide more energy to the increasing global electrical energy demand. Most of the distribution power sources provide clean energy compared to traditional fossil fuel and can also provide sufficient power for the load with a large enough distribution power plant. However, distributed energy could also cause problems. Distribution energy sources, such as solar and wind are not stable and highly dependent on weather condition, they cannot be scheduled to follow the demand change. The power generated from renewable energy sources can impact the distribution grid [1]. Either the grid frequency or the voltage magnitude. In this situation the active and reactive power support is necessary. The frequency regulation can be achieved through active power control, while the magnitude regulation is controlled by reactive power. Distribution energy can be better utilized in microgrid rather than in a traditional power grid.

Microgrid is a new type of power grid, providing an efficient and smart way to supply energy. A microgrid contains groups of local power sources, loads, and storage. It can connect to the conventional grid or operate as an independent system. Figure 1.1 shows a microgrid model, where the microgrid connected to the utility grid through a switch. The energy sources

can be wind, solar, energy storage system or other distributed generation. That means microgrid can be disconnected from the traditional grid and operate in islanded mode at the time of need. With distributed generation, a microgrid can provide energy to support the utility grid in connected mode.

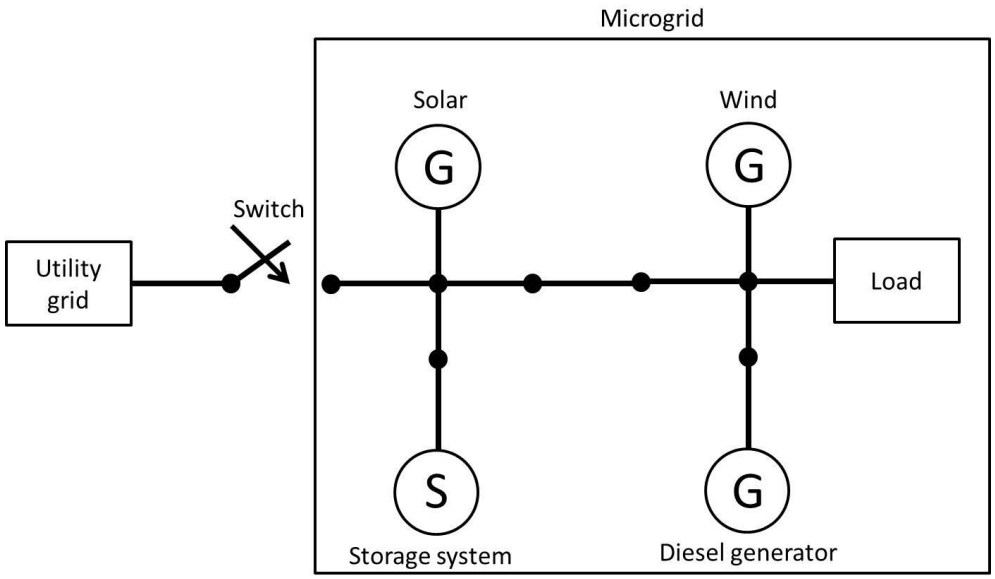

Figure 1. 1 Microgrid model

Providing the power from a distributed energy usually leads to a better energy efficiency due to the reduction of transmission losses. The distributed energy can be connected quickly and not limited by transmission and distribution systems. Higher penetration of distributed energy means the microgrid is more likely to suffer from the instability of distributed energy sources. Keeping the power system stable is an important issue. Storage systems play vital roles in microgrids in maintaining the stability. Storage systems can be placed in a microgrid

to regulate voltage and frequency; and can absorb energy during low load demand and discharge while the load demand soars.

The growing penetration of wind turbines in the grid leads to the instability of frequency. The absence of synchronization torque for variable-speed wind generators causes the decreases in overall system inertia, as well as the reduction of frequency regulation capabilities [2]. The active power support from energy storage provides frequency regulation.

With high photovoltaic (PV) penetration rates, solar power generation will produce some negative impacts on the system, such as voltage rise and fluctuation, and reverse power flow [3]. The reactive power support can mitigate the negative impacts from the high PV penetration.

Storage systems are expensive, it is impossible to have a storage unit install everywhere in the grid. Connecting a storage system randomly to the grid would not have the best performance. It is necessary to identify a location that the storage system can impact and regulate the system efficiently.

The objective of this study is to find the optimal location for a storage system in a straightforward and fast way. To identify the optimal location of storages, the sensitivity indices are proposed. The sensitivity indices are based on the Jacobian matrix, obtained by the Newton-Raphson method. The sensitivity indices can be calculated from the inverse of Jacobian matrix. The effect of active and reactive powers at voltage magnitude and angle can

be studied through the sensitivity indices. The details of the Newton-Raphson method and sensitivity indices will be discussed in chapter three.

The indices will reveal the information about how well a node can impact the whole system with active and reactive power injection. The sensitivity indices considered the Nodes with high indices values as a suitable location for the storage system. Nodes with lower sensitivity indices have a lower impact on the voltage angle and magnitude in the system. The evaluation of indices will be present in chapter four.

CHAPTER 2 LITERATURE REVIEW

The topics of interest in this study including the distributed generation and its impacts, voltage angle stability, sensitivity analysis and the optimal placement are presented here.

2. 1 Distribute Generation

Distributed Generation (DG) refers to electric power generation within distribution networks or on the customer side of the network [4]. DG consists of many small energy sources connected to a distribution system. The energy sources in DG could be generator or energy storage system. DG can be categorized as below:

Conventional generator

- Gas or steam turbine based synchronous generator
- Diesel generator

Non-Conventional Generators

- Storage Devices
- Solar-based inverter
- Wind turbine based doubly fed induction generator
- Wind turbine based constant speed squirrel cage induction generator
- Wind turbine based permanent magnet synchronous generator

DG provides benefits for energy efficiency of distribution systems, such as environmental pollution reduction and enhanced system reliability [5]. The advantages of DGs in a power system are:

- Minimizing Power Losses
- Voltage Profile Improvement
- Voltage Stability
- Reliability
- Power Quality

The approach to determine the optimal DG-unit's size, power factor and location to minimize the total system real power loss is proposed in [6]. The reliability of DG in distribution systems is studied in [7]. Residential renewable energy generator is a common type of DG for power network support, due to its small scale and easy to install. Renewable DG can be installed in household, factories, offices and distributed system. Extra energy generation can send back to the distribution network and support demand in the grid. Energy storage system in DG can also mitigate the intermittency, provides system security, reliability, and energy arbitrage [8].

Energy storage systems eable higher penetration of renewable energy systems such as splar and wind energy, by mitigating their instability. Combining the wind power generation system with energy storage will reduce the fluctuation of wind power [9]. The storage system

can also be used to smooth out the fluctuation of PV system caused by cloud passing [10]. Another advantage of energy storage system is the ability of apply voltage and frequency control with the support of active and reactive power. Because of the price of storage systems are high, it is necessary to select a highly effectve location for energy storage system. Choosing a random location will not necessarily lead to the best efficiency.

The demand for clear and substantial energy calls for an increasing penetration of renewable energy in power systems. A microgrid is a cluster of DGs place in the system to provide power to the local load [11], the sources of energy could be renewable. Contrary to the traditional grid, the microgrid can operate in islanded mode in case of grid power outage. Some microgrids could have a high penetration of renewable energy source for lower carbon emission, but high penetration of renewable energy source may cause power reliability and quality problems. The DG placement strategies for grid reinforcement is discussed in [12]. Selection of the best location and size of DGs provide power loss reduction and voltage profile enhancement. As an example of a typical microgrid, Figure 2.1 shows the configuration of the standard IEEE 34-node microgrid from the site of the Power Energy Society (PES) [13].

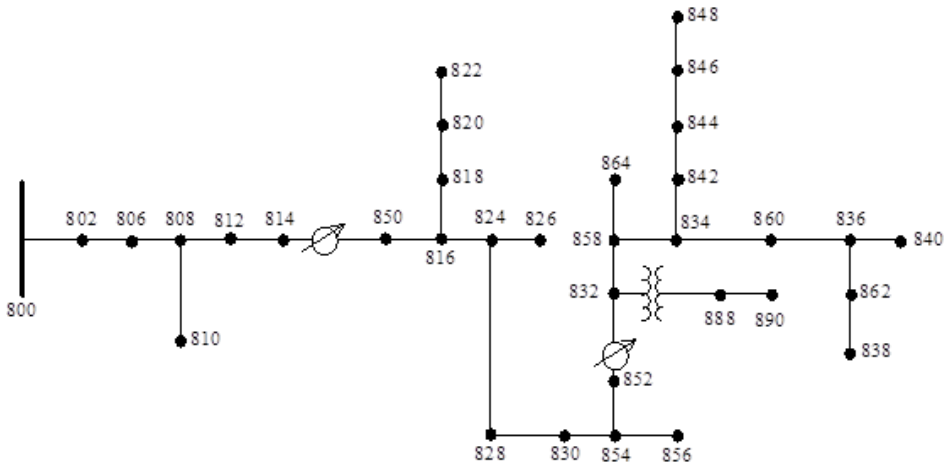

Figure 2. 1 IEEE 34-node system

The IEEE 34-node system is an existing testing feeder located in Arizona with two regulators, a transformer and operates at voltage value 24.9 kV. Load types includes PQ loads and impedance loads in forms of three-phase, two-phase and single-phase.

2. 2 Voltage Angle Stability

The active and reactive power support from storage system can stabilize both of the angle and voltage profiles in the distribution system. In [14], the impacts of large-scale wind power penetration on the angle and voltage stability are discussed. The study analyzed the changing nature of power system's behavior under large-scale wind turbine in some cases. Reference [15] focuses on the impact of PV installation on the short term voltage stability. PV severely impairs the short-term voltage stability when power is shutted off afer a voltage sag. Operating the PV system at leading a power factor and deploying PV equipment with the

ability to inject reactive current by the PV inverters would improve the short-term voltage stability.

To enhance system stability, [16] presents a new reactive power loss index for identifying the weak buses in the system. The index can be used to select the optimal location for reactive compensation devices, which provides reactive power support to prevent the voltage collapse. The index computed from the reactive power support and loss allocation algorithm using the Y-bus method. The fuzzy logic approach is used to identify the most severe network line outages in the system. The benefit of this approach is that the index is obtained without iterations, the other existing methods need iteration to approach the weak buses.

A method to utilize the DG units to improve the voltage stability margin is proposed in [17]. It selected the candidate buses for the DG unit installation with voltage sensitivity analysis. A reduced Jacobian matrix is calculated to analyze the sensitivity of voltage magnitude variations to active power injection. The nodes with high sensitivity are considered as the candidate buses. The method only concerns the sensitivity of voltage magnitude to active power injection in the candidate buses selection process. The voltage angle has not been considered in this paper. Also, PV bus is not being considered in this reference.

A major advantage of the storage systems is the fast and accurate active power control. Reference [18] utilized a small-scale battery energy storage system to eliminate the secondary frequency drop issue during the rotor speed restoration of the permanent magnet synchronous generator wind turbine generator. The storage system provided frequency regulation on demand and discontinue when the system frequency is restored to the specified value.

2. 3 Jacobian-Based Sensitivity Analysis

The Jacobian matrix is a natural by-product of the Newton-Raphson load flow algorithm [19]. It is obtained by solving the equation (2.1) iteratively.

$$\begin{bmatrix} \Delta \mathrm{P} \\ \Delta \mathrm{Q} \end{bmatrix} = J \begin{bmatrix} \Delta \delta \\ \Delta V \end{bmatrix} \tag{2.1}$$

Where ΔP and ΔQ are the active and reactive power mismatch at each bus. J is the Jacobian matrix, represents the sensitivity measurement of the active and reactive power on the bus voltage angle and magnitude. $\Delta\delta$ and ΔV are the corrections of the voltage angle and magnitude. With the updated of voltage angle and magnitude in each step of the iteration, ΔP and ΔQ calculated at each iteration. The process of iteration will continue until ΔP and ΔQ are falling in certain tolerance threshold.

One problem of the Newton-Raphson power flow is that the iteration fails to converge when the smallest singular value of the Jacobian matrix becomes too small. A methodology of Jacobian matrix improvement by directly eliminate the singularity [12]. Continuation

power flow methods developed to solve the ill-condition in conventional Newton-Raphson power flow Jacobian matrix.

There are numbers of research study the sensitivity based on the Jacobian matrix. Reference [20] introduces a software ElecNetKit (Electric Network Toolkit) that simplifies the development of voltage management strategies with sensitivity analysis. The research focuses on the sensitivity of voltage magnitude to active and reactive power. Perturb-and-observe method is used when the Jacobian matrix is not available, the method makes small modifications of active and reactive powers and measures the impact on voltage magnitude. ElecNetKit can interface with OpenDSS, an open-source distribution systems simulator package developed by the Electric Power Research Institute (EPRI). It takes OpenDSS models as a starting point to fully develop the project. The perturb-and-observe network algorithm is applied to get sensitivities because the Jacobian matrix is unavailable in OpenDSS. The method generated sensitivities of the voltage magnitude at various buses by changes active and reactive powers. Afterward, the method is validated with Newton-Raphson load flow algorithm written in MATLAB. One major drawback of this approach is that the sensitivity data is obtained through the perturb-and-observe method and it is time-consuming, especially for the large system.

Reference [21] presents a reactive power control method for PV systems to mitigate the voltage fluctuations base on voltage sensitivity analysis. The variations in the voltage

magnitude of buses are concerned. The required reactive power adjustment to compensate the voltage fluctuations is calculated from the Jacobian matrix.

2. 4 Optimal Placement of Storage

The connection of DGs could create negative impact to the system. The key issues related to optimal placement and sizing of DG have been discussed in [22]. The key issues related to DG are:

- Distribution process and planning issues:

  Local protection systems need to be adopted for distributed generation connection.

- Distribution network issues:

  Distribution systems are usually not designed to connect to distributed generation.

- Power quality:

  Distributed generators connected to distribution systems might cause some power quality issues.

- Power reserve and balancing

  The Distribution System Operator must be able to manage fast reacting local power generation and in some cases procure the needed power reserve from the upstream transmission.

- Connection issues

There are problems in connecting various distributed generatiors to conventional centralized power generation.

The energy storage system has become one of the most viable solutions for facilitating increased penetration of renewable DG resources. Reference [23] - [25] are focused on increasing the penetration of renewable energy with the optimal energy storage systems placement. Reference [23] proposed a flywheel energy storage that provides primary frequency regulation. An optimal location for the deployment of energy storage system can be found with small-signal stability analysis and time-domain simulations. In reference [24], a methodology is proposed for optimally allocating energy storage systems in distribution systems under a high penetration of wind energy. The energy storage system in the system is to minimize the annual electricity cost. Reference [25] indicated that energy storage over 10 minutes using flywheel allows 10% more wind energy to be absorbed without grid reinforcement and 24 hours using redox flow cells allows up to 25% more wind energy to be absorbed. Together, these studies indicate that energy storage systems provide benefits to the system with renewable DG resources.

The optimal location for the storage system is to reach the best performance. There is some evidence to suggest that the location of the storage system influences the performance significantly. The impacts of different storage technologies on the economic dispatch of a distribution system is studied in reference [26]. The study suggested that the optimal location

of the storage has a significant impact on the minimization of the operational cost instant of increase in size and the type of storage technology. Reference [27] model a distribution network as a continuous tree with the linearized DistFlow model by solving the power flow equations. The approach demonstrates that storage devices should be placed near the leaves of the network and far from the substation and the storage will have better performance on loss reduction. These studies indicate that the performance of energy storage highly depends on the location.

The method to select the optimal placement of storage system has drawn particular attention in many studies. The method of optimal placement of DGs and storage devices for improving system transient stability has been discussed in [28] - [33]. Reference [28] proposes a novel approach for the optimal placement of energy storage devices based on microgrid structure preserving energy function. The purpose of the approach is to improve microgrid transient stability. Fault scan is using fault critical clearing time as the key index to find the most serious fault case and then calculating microgrid branch transient energy function to identify the optimal installation position for energy storage.

References [29] and [30] considered the optimal location to reducing the transmission network congestion. [29] proposed a program that determines the optimal location and the size of a storage device, which is placed to store extra energy from renewable sources for later usage and to reduce the transmission network congestion. The method focused on

reducing the system-wide operating cost and the cost of investments in energy storage. The minimum profit constraint influences the optimal storage placing and sizing. Reference [30] proposed a three-stage decomposition of the problem and considered both the economic and technical aspects. The location and distribution of storage are dependent on the distribution of wind resources.

Reference [31] formulated the optimal storage placement problem for load shifting at slow time scales. The study focused on minimizing the cost of conventional generation by load shifting with energy storage devices, the method in [31] smooths the generation curve rather than following the load variations.

The approach for optimal placement of the battery energy storage system in the distribution system to reduce the distribution system losses is proposed in [32]. The loss sensitivity index is generated through considering the changes in the power system performance and the battery energy storage system parameters. The Newton-Raphson iterative technique has been used to solve the power flow. Bus voltages, voltage phase angles, and the power flows are obtained for sensitivity index. Result shows that battery energy storage system can reduce losses in the system during charging mode.

Both [33] and [34] located the optimal location based on Genetic Algorithms (GA). Reference [33] is finding the optimal locations and capacities of energy storage systems for power system vulnerability mitigation. The vulnerability assessment is proposed to calculate

the impact factors for power systems based on generator and line outages. The optimal locations and capacities for energy storage systems placement are derived and solved by a genetic algorithm-based method. The buses with larger bus impact severity value are considered as better locations for energy storage systems. Reference [34] proposed a method based on GA for optimal placement of DG units. Maximize the loadability of reactive power capabilities. The algorithm obtained the reactive power injected and DG bus location for optimal placement. Due to the iterative process in the genetic algorithm-based method, more computational time is required for the larger system.

In the view of decreasing system cost with DGs connection, the optimal placement of energy storage systems also concerned. Reference [35] minimize the power system cost and improve the system voltage profiles with optimal location and sizing under the consideration of uncertainties in wind power production. The method searched the minimum cost and voltage deviation iteratively. [36] determining the best location for installation of the energy storage systems for daily operation. The process of iteration is done for every bus of the network to find the best location for installation of the storage system.

2.6 Conclusion

The process of iteration has been widely used for the optimal placement of storage system. In [32], iteration is used in the genetic algorithm-based method. Reference of [29]

formalize and construct the storage budget and demand problem for optimal location iteratively, sizing and control of storage devices in a power network. In references [36] and [37], iteration is used to approach minimum cost. Due to the iterative process, selecting optimal location for storage system in the larger system would be more challenging and time-consuming. Moreover, there would be some limitation in the method to reach the converged state in the iterative process.

CHAPTER 3 JACOBIAN MATRIX AS A SENSITIVITY ANALYSIS TOOL

3. 1 Power flow analysis

Power flow analysis is one of the most common methods of planning and designing in power systems. The power flow study is to obtain the voltage magnitude and angle of the at each bus and the real and reactive power flow in each line [19]. In power flow analysis, there are three types of buses that can be classified.

- Load buses (PQ): A non-generator bus or load bus is often called a PQ bus. Voltage angle (δ) and magnitude ($|V|$) are unknown. Power generated (P_G, Q_G) are zero, power drawn by the load (P_L, Q_L) are known. Mismatches $\triangle$P and ΔQ can be defined.
- Voltage-controlled buses (PV): Bus with generator connected that $|V|$ is kept constant, P_G is specified. Q_G cannot be known in advance so mismatch ΔQ cannot be defined, δ is unknown as well.
- Slack buses (Swing): Bus which δ serves as reference for the angles of all other bus voltages, and $|V|$ is specified.

The following table shows the characteristic of each bus types.

Table 3. 1 Types of bus

Bus type	Unknown	Known
PQ bus	$\delta, \lvert V \rvert$	P, Q
PV bus	δ, Q	$\lvert V \rvert, P$
Slack bus	P, Q	$\delta, \lvert V \rvert$

Power flow analysis is similar to circuit analysis except that the power flow analysis is nonlinear and circuit analysis is linear. The equation of power flow complex matrix is:

$$I = Y_{bus}V \tag{3. 1}$$

Where Y_{bus} is the bus admittance matrix, V is the complex node voltage vector, I is the nodal current injection vector. In Y_{bus} matrix, the typical element Y_{in} are:

$$Y_{ij} = |Y_{in}|\angle\theta_{in} = |Y_{in}|\, cos\, \theta_{in} + j|Y_{in}|\, sin\, \theta_{in} = G_{in} + jB_{in} \tag{3. 2}$$

The voltage at a bus *i* can be obtained using:

$$V_i = |V_i|\angle\theta_i = |V_i|(\cos\delta_i + j\sin\delta_i) \tag{3. 3}$$

The net current injected into the network at bus *i* in terms of the elements Y_{in} in Y_{bus} is given in:

$$I_i = Y_{i1}V_1 + Y_{i2}V_2 + \cdots + Y_{iN}V_N = \sum_{n=1}^{N} Y_{in}V_n \tag{3. 4}$$

The complex conjugate of the power injected at bus *i* is:

$$S_i = V_i^* I_i = V_i^* \sum_{n=1}^{N} Y_{in} V_n \tag{3. 5}$$

Substituting from equations (3.4) and (3.5) and obtain:

$$S_i = \sum_{n=1}^{N} |Y_{in} V_i V_n| \angle(\theta_{in} + \delta_n - \delta_i) \tag{3. 6}$$

Separating the equation into real and reactive parts and the equations obtain:

$$P_i = \sum_{n=1}^{N} |Y_{in} V_i V_n| \, cos(\theta_{in} + \delta_n - \delta_i) \tag{3. 7}$$

$$Q_i = -\sum_{n=1}^{N} |Y_{in} V_i V_n| \, sin(\theta_{in} + \delta_n - \delta_i) \tag{3. 8}$$

Then,

$$P_{i.sch} = P_{iG} - P_{iL} \tag{3. 9}$$

$P_{i.sch}$ is the net scheduled power being injected in to the network at bus i, $P_{i.clc}$ is the calculated value of P_i. The definition of mismatch ΔP is $P_{i.sch}$ minus $P_{i.clc}$.

$$\Delta P = P_{i.sch} - P_{i.clc} \tag{3. 10}$$

Therefore, the reactive power mismatch ΔQ is:

$$\Delta Q = Q_{i.sch} - Q_{i.clc} \tag{3. 11}$$

3. 2 Newton-Raphson load flow

The Newton-Raphson method is to obtain the Jacobian matrix. To apply the method, set bus voltages and line admittances in polar form and get:

$$P_i = |V_i|^2 G_{ii} + \sum_{\substack{n=1 \\ n \neq i}}^{N} |Y_{in} V_i V_n| \cos(\theta_{in} + \delta_n - \delta_i) \tag{3. 12}$$

$$Q_i = -|V_i|^2 B_{ii} - \sum_{\substack{n=1 \\ n \neq i}}^{N} |Y_{in} V_i V_n| \sin(\theta_{in} + \delta_n - \delta_i) \tag{3. 13}$$

G_{ii} and B_{ii} come from the definition of Y_{ij} in equation (3.2). The real and reactive power mismatches for bus *i* is:

$$\Delta P_i = P_{i.sch} - P_{i.clc} \tag{3. 14}$$

$$\Delta Q_i = Q_{i.sch} - Q_{i.clc} \tag{3. 15}$$

Power flow calculations usually employ iterative techniques such as the Newton-Raphson procedures. At each interval, $P_{i.sch}$ and $Q_{i.sch}$ are being calculated based on the estimated δ_i and $|V_i|$ from equations (3. 12) – (3. 13). Then mismatches ΔP_i and ΔQ_i need to be calculated from equations (3. 14) – (3. 15). By Comparing the calculated values with the known values the errors are being generated and from the error the new estimations of values of δ_i and $|V_i|$ are being derived as the starting values for the next iteration. At each iteration, the real and reactive power have to be within specified tolerances.

The Jacobian sub-matrices are being calculated and triangularized in each iteration to update the Jacobian matrix. The Newton-Raphson method calculates mismatches until real and reactive power mismatches at all buses fall within specified tolerances. Figure 3.1 is the diagram of the Newton-Raphson iteration process.

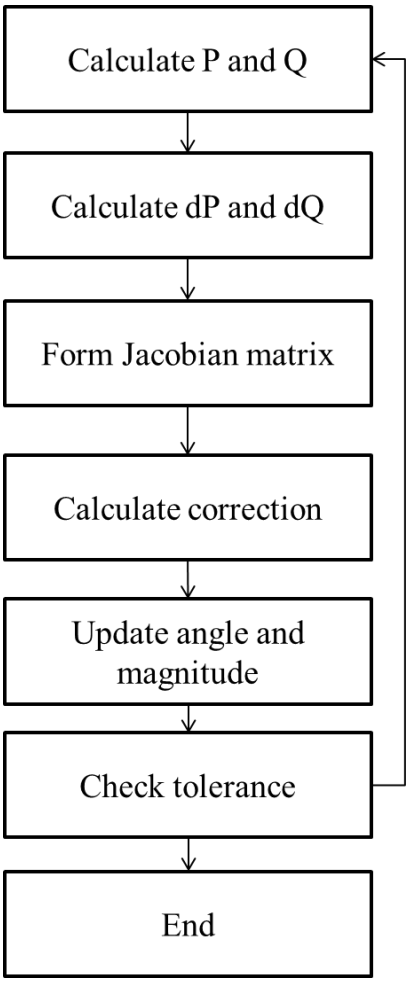

Figure 3. 1 Diagram of the Newton-Raphson iteration process

In the diagram, P and Q are bus real and reactive power. dP and dQ are real and reactive power mismatches for each bus. The tolerance value could be in the range of 10^{-3} to 10^{-7}.

The Jacobian matrix of n buses system has the structure below:

$$\begin{bmatrix} \Delta \mathrm{P} \\ \Delta \mathrm{Q} \end{bmatrix} = \begin{bmatrix} \frac{\partial P}{\partial \delta} & \frac{\partial P}{\partial V} \\ \frac{\partial Q}{\partial \delta} & \frac{\partial Q}{\partial V} \end{bmatrix} \begin{bmatrix} \Delta \delta \\ \Delta \mathrm{V} \end{bmatrix} \tag{3. 16}$$

Where $\Delta \mathrm{P}$ and $\Delta \mathrm{Q}$ are the real and reactive power mismatch, the Jacobian matrix is the middle part of the equation which represents the sensitivity measurement of the real and reactive power on the bus voltage angle and magnitude. The Jacobian matrix for a N-bus system has shown in equation (3. 17).

$$\begin{bmatrix} \Delta P_2 \\ \Delta P_3 \\ \vdots \\ \Delta P_N \\ \Delta Q_2 \\ \Delta Q_3 \\ \vdots \\ \Delta Q_N \end{bmatrix} = \begin{bmatrix} J_1 & J_2 \\ J_3 & J_4 \end{bmatrix} \begin{bmatrix} \Delta \delta_2 \\ \Delta \delta_2 \\ \vdots \\ \Delta \delta_N \\ \Delta |V_2| \\ \Delta |V_3| \\ \vdots \\ \Delta |V_N| \end{bmatrix} \tag{3. 17}$$

The mismatches for the slack bus does not including, since ΔP_1 and ΔQ_1 are undefined with P_1 and Q_1 are not scheduled. $\Delta \delta_1$ and $\Delta |V_1|$ are also not including, when corrections of angle and magnitude are both zero at the slack bus. The groups of J_1, J_2, J_3, and J_4 are:

$$J_1 = \begin{bmatrix} \frac{\partial P_2}{\partial \delta_2} & \frac{\partial P_2}{\partial \delta_3} & \cdots & \frac{\partial P_2}{\partial \delta_N} \\ \frac{\partial P_3}{\partial \delta_2} & \frac{\partial P_3}{\partial \delta_3} & \cdots & \frac{\partial P_3}{\partial \delta_N} \\ \vdots & \vdots & \ddots & \vdots \\ \frac{\partial P_N}{\partial \delta_2} & \frac{\partial P_N}{\partial \delta_3} & \cdots & \frac{\partial P_N}{\partial \delta_N} \end{bmatrix} \quad (3.\ 18)$$

$$J_2 = \begin{bmatrix} \frac{\partial P_2}{\partial |V_2|} & \frac{\partial P_2}{\partial |V_3|} & \cdots & \frac{\partial P_2}{\partial |V_N|} \\ \frac{\partial P_3}{\partial |V_2|} & \frac{\partial P_3}{\partial |V_3|} & \cdots & \frac{\partial P_3}{\partial |V_N|} \\ \vdots & \vdots & \ddots & \vdots \\ \frac{\partial P_N}{\partial |V_2|} & \frac{\partial P_N}{\partial |V_3|} & \cdots & \frac{\partial P_N}{\partial |V_N|} \end{bmatrix} \quad (3.\ 19)$$

$$J_3 = \begin{bmatrix} \frac{\partial Q_2}{\partial \delta_2} & \frac{\partial Q_2}{\partial \delta_3} & \cdots & \frac{\partial Q_2}{\partial \delta_N} \\ \frac{\partial Q_3}{\partial \delta_2} & \frac{\partial Q_3}{\partial \delta_3} & \cdots & \frac{\partial Q_3}{\partial \delta_N} \\ \vdots & \vdots & \ddots & \vdots \\ \frac{\partial Q_N}{\partial \delta_2} & \frac{\partial Q_N}{\partial \delta_3} & \cdots & \frac{\partial Q_N}{\partial \delta_N} \end{bmatrix} \quad (3.\ 20)$$

$$J_4 = \begin{bmatrix} \frac{\partial Q_2}{\partial |V_2|} & \frac{\partial Q_2}{\partial |V_3|} & \cdots & \frac{\partial Q_2}{\partial |V_N|} \\ \frac{\partial Q_3}{\partial |V_2|} & \frac{\partial Q_3}{\partial |V_3|} & \cdots & \frac{\partial Q_3}{\partial |V_N|} \\ \vdots & \vdots & \ddots & \vdots \\ \frac{\partial Q_N}{\partial |V_2|} & \frac{\partial Q_N}{\partial |V_3|} & \cdots & \frac{\partial Q_N}{\partial |V_N|} \end{bmatrix} \quad (3.\ 21)$$

By collecting equations (3. 17) – (3. 20) and putting them back to (3. 16), we obtain:

$$\begin{bmatrix} \Delta P_2 \\ \Delta P_3 \\ \vdots \\ \Delta P_N \\ \Delta Q_2 \\ \Delta Q_3 \\ \vdots \\ \Delta Q_N \end{bmatrix} = \begin{bmatrix} \frac{\partial P_2}{\partial \delta_2} & \frac{\partial P_2}{\partial \delta_3} & \cdots & \frac{\partial P_2}{\partial \delta_N} & \frac{\partial P_2}{\partial |V_2|} & \frac{\partial P_2}{\partial |V_3|} & \cdots & \frac{\partial P_2}{\partial |V_N|} \\ \frac{\partial P_3}{\partial \delta_2} & \frac{\partial P_3}{\partial \delta_3} & \cdots & \frac{\partial P_3}{\partial \delta_N} & \frac{\partial P_3}{\partial |V_2|} & \frac{\partial P_3}{\partial |V_3|} & \cdots & \frac{\partial P_3}{\partial |V_N|} \\ \vdots & \vdots & \ddots & \vdots & \vdots & \vdots & \ddots & \vdots \\ \frac{\partial P_N}{\partial \delta_2} & \frac{\partial P_N}{\partial \delta_3} & \cdots & \frac{\partial P_N}{\partial \delta_N} & \frac{\partial P_N}{\partial |V_2|} & \frac{\partial P_N}{\partial |V_3|} & \cdots & \frac{\partial P_N}{\partial |V_N|} \\ \frac{\partial Q_2}{\partial \delta_2} & \frac{\partial Q_2}{\partial \delta_3} & \cdots & \frac{\partial Q_2}{\partial \delta_N} & \frac{\partial Q_2}{\partial |V_2|} & \frac{\partial Q_2}{\partial |V_3|} & \cdots & \frac{\partial Q_2}{\partial |V_N|} \\ \frac{\partial Q_3}{\partial \delta_2} & \frac{\partial Q_3}{\partial \delta_3} & \cdots & \frac{\partial Q_3}{\partial \delta_N} & \frac{\partial Q_3}{\partial |V_2|} & \frac{\partial Q_3}{\partial |V_3|} & \cdots & \frac{\partial Q_3}{\partial |V_N|} \\ \vdots & \vdots & \ddots & \vdots & \vdots & \vdots & \ddots & \vdots \\ \frac{\partial Q_N}{\partial \delta_2} & \frac{\partial Q_N}{\partial \delta_3} & \cdots & \frac{\partial Q_N}{\partial \delta_N} & \frac{\partial Q_N}{\partial |V_2|} & \frac{\partial Q_N}{\partial |V_3|} & \cdots & \frac{\partial Q_N}{\partial |V_N|} \end{bmatrix} \begin{bmatrix} \Delta \delta_2 \\ \Delta \delta_2 \\ \vdots \\ \Delta \delta_N \\ \Delta |V_2| \\ \Delta |V_3| \\ \vdots \\ \Delta |V_N| \end{bmatrix} \quad (3.\ 22)$$

The dimension of the Jacobian matrix is decided by the number of PV bus and PQ bus. At PQ buses, both angle and magnitude are existing. At PV bus, the magnitude is kept constant and only angle existing in the matrix. If bus *N* is defined as PV bus, the Jacobian matrix will be reduced as:

$$\begin{bmatrix} \Delta P_2 \\ \Delta P_3 \\ \vdots \\ \Delta P_N \\ \Delta Q_2 \\ \Delta Q_3 \\ \vdots \\ \Delta Q_{N-1} \end{bmatrix} = \begin{bmatrix} \frac{\partial P_2}{\partial \delta_2} & \frac{\partial P_2}{\partial \delta_3} & \cdots & \frac{\partial P_2}{\partial \delta_N} & \frac{\partial P_2}{\partial |V_2|} & \frac{\partial P_2}{\partial |V_3|} & \cdots & \frac{\partial P_2}{\partial |V_{N-1}|} \\ \frac{\partial P_3}{\partial \delta_2} & \frac{\partial P_3}{\partial \delta_3} & \cdots & \frac{\partial P_3}{\partial \delta_N} & \frac{\partial P_3}{\partial |V_2|} & \frac{\partial P_3}{\partial |V_3|} & \cdots & \frac{\partial P_3}{\partial |V_{N-1}|} \\ \vdots & \vdots & \ddots & \vdots & \vdots & \vdots & \ddots & \vdots \\ \frac{\partial P_N}{\partial \delta_2} & \frac{\partial P_N}{\partial \delta_3} & \cdots & \frac{\partial P_N}{\partial \delta_N} & \frac{\partial P_N}{\partial |V_2|} & \frac{\partial P_N}{\partial |V_3|} & \cdots & \frac{\partial P_N}{\partial |V_{N-1}|} \\ \frac{\partial Q_2}{\partial \delta_2} & \frac{\partial Q_2}{\partial \delta_3} & \cdots & \frac{\partial Q_2}{\partial \delta_N} & \frac{\partial Q_2}{\partial |V_2|} & \frac{\partial Q_2}{\partial |V_3|} & \cdots & \frac{\partial Q_2}{\partial |V_{N-1}|} \\ \frac{\partial Q_3}{\partial \delta_2} & \frac{\partial Q_3}{\partial \delta_3} & \cdots & \frac{\partial Q_3}{\partial \delta_N} & \frac{\partial Q_3}{\partial |V_2|} & \frac{\partial Q_3}{\partial |V_3|} & \cdots & \frac{\partial Q_3}{\partial |V_{N-1}|} \\ \vdots & \vdots & \ddots & \vdots & \vdots & \vdots & \ddots & \vdots \\ \frac{\partial Q_{N-1}}{\partial \delta_2} & \frac{\partial Q_{N-1}}{\partial \delta_3} & \cdots & \frac{\partial Q_{N-1}}{\partial \delta_N} & \frac{\partial Q_{N-1}}{\partial |V_2|} & \frac{\partial Q_{N-1}}{\partial |V_3|} & \cdots & \frac{\partial Q_{N-1}}{\partial |V_{N-1}|} \end{bmatrix} \begin{bmatrix} \Delta \delta_2 \\ \Delta \delta_2 \\ \vdots \\ \Delta \delta_N \\ \Delta |V_2| \\ \Delta |V_3| \\ \vdots \\ \Delta |V_{N-1}| \end{bmatrix} \quad (3.\ 23)$$

The size of Jacobian matrix can be calculated as:

$$J_{(npv+2npq)\times(npv+2npq)} \quad (3.\ 24)$$

Where *npv* is the number of PV bus and *npq* is number of PQ bus. The size of J_1, J_2, J_3, and J_4 are:

$$J_{1(npv+npq)\times(npv+npq)} \quad (3.\ 25)$$

$$J_{2(npv+npq)\times(npq)} \quad (3.\ 26)$$

$$J_{3(npq)\times(npv+npq)} \quad (3.\ 27)$$

$$J_{4(npq)\times(npq)} \quad (3.\ 28)$$

3. 3 Sensitivity analysis

While the power flow equations are solved and Jacobian matrix obtained. The inverse of the Jacobian matrix can be calculated, and the matrix has the following structure:

$$\begin{bmatrix} \Delta\delta_2 \\ \Delta\delta_2 \\ \vdots \\ \Delta\delta_N \\ \Delta|V_2| \\ \Delta|V_3| \\ \vdots \\ \Delta|V_N| \end{bmatrix} = \begin{bmatrix} \frac{\partial\delta_2}{\partial P_2} & \frac{\partial\delta_2}{\partial P_3} & \cdots & \frac{\partial\delta_2}{\partial P_n} & \frac{\partial\delta_2}{\partial Q_2} & \frac{\partial\delta_2}{\partial Q_3} & \cdots & \frac{\partial\delta_2}{\partial Q_N} \\ \frac{\partial\delta_3}{\partial P_2} & \frac{\partial\delta_3}{\partial P_3} & \cdots & \frac{\partial\delta_3}{\partial P_n} & \frac{\partial\delta_3}{\partial Q_2} & \frac{\partial\delta_3}{\partial Q_3} & \cdots & \frac{\partial\delta_3}{\partial Q_N} \\ \vdots & \vdots & \ddots & \vdots & \vdots & \vdots & \ddots & \vdots \\ \frac{\partial\delta_N}{\partial P_2} & \frac{\partial\delta_N}{\partial P_3} & \cdots & \frac{\partial\delta_N}{\partial P_n} & \frac{\partial\delta_N}{\partial Q_2} & \frac{\partial\delta_N}{\partial Q_3} & \cdots & \frac{\partial\delta_N}{\partial Q_n} \\ \frac{\partial|V_2|}{\partial P_2} & \frac{\partial|V_2|}{\partial P_3} & \cdots & \frac{\partial|V_2|}{\partial P_n} & \frac{\partial|V_2|}{\partial Q_2} & \frac{\partial|V_2|}{\partial Q_3} & \cdots & \frac{\partial|V_2|}{\partial Q_n} \\ \frac{\partial|V_3|}{\partial P_2} & \frac{\partial|V_3|}{\partial P_3} & \cdots & \frac{\partial|V_3|}{\partial P_n} & \frac{\partial|V_3|}{\partial Q_2} & \frac{\partial|V_3|}{\partial Q_3} & \cdots & \frac{\partial|V_3|}{\partial Q_N} \\ \vdots & \vdots & \ddots & \vdots & \vdots & \vdots & \ddots & \vdots \\ \frac{\partial|V_N|}{\partial P_2} & \frac{\partial|V_N|}{\partial P_3} & \cdots & \frac{\partial|V_N|}{\partial P_n} & \frac{\partial|V_N|}{\partial Q_2} & \frac{\partial|V_N|}{\partial Q_3} & \cdots & \frac{\partial|V_N|}{\partial Q_N} \end{bmatrix} \begin{bmatrix} \Delta P_2 \\ \Delta P_3 \\ \vdots \\ \Delta P_N \\ \Delta Q_2 \\ \Delta Q_3 \\ \vdots \\ \Delta Q_N \end{bmatrix} \quad (3.\ 29)$$

The inverse Jacobian matrix can also separate into four sub-matrices, J_1^{-1}, J_2^{-1}, J_3^{-1}, and J_4^{-1}. The structure of four sub-matrices in inverse Jacobian Matrix has shown in equation (3. 30).

$$\begin{bmatrix} \Delta\delta \\ \Delta\mathrm{V} \end{bmatrix} = \begin{bmatrix} J_1^{-1} & J_2^{-1} \\ J_3^{-1} & J_4^{-1} \end{bmatrix} \begin{bmatrix} \Delta\mathrm{P} \\ \Delta\mathrm{Q} \end{bmatrix} \quad (3.\ 30)$$

In the case that only one slack bus and PQ buses existing in the system, the size of four sub-matrices are equal. However, if PV bus exists in the system, the sizes are not equal. For

example, there is a system with four buses that is one slack bus, one PV bus, and two PQ buses. From equation (3.25) – (3.28) the size of the Jacobian matrix is:

$$J_{(5)\times(5)}$$

For the sub-matrices of J_1, J_2, J_3, and J_4, the size are:

$$J_{1(3)\times(3)}$$

$$J_{2(3)\times(2)}$$

$$J_{3(2)\times(3)}$$

$$J_{4(2)\times(2)}$$

Similarly, inverse Jacobian matrix, the size of four sub-matrices are different. For the optimal location for storage, PV buses are not considered as the potential candidates. Values in the matrices that content PV buses elements need to be removed from the matrices. While only PQ elements exist in J_4^{-1}, the rest of them, J_1^{-1}, J_2^{-1} and J_3^{-1}, all include PV bus elements in their matrices.

The example of remove PV bus elements is demonstrated, the PV bus is set at bus 4. The inverse of Jacobian matrix is shown in Table 3.2 where color distinguishes four sub-matrices.

Table 3. 2 Inverse Jacobian matrix of 4 buses

$\frac{\partial \delta_2}{\partial \mathrm{P}_2}$	$\frac{\partial \delta_2}{\partial \mathrm{P}_3}$	$\frac{\partial \delta_2}{\partial \mathrm{P}_4}$	$\frac{\partial \delta_2}{\partial Q_2}$	$\frac{\partial \delta_2}{\partial Q_3}$
$\frac{\partial \delta_3}{\partial \mathrm{P}_2}$	$\frac{\partial \delta_3}{\partial \mathrm{P}_3}$	$\frac{\partial \delta_3}{\partial \mathrm{P}_4}$	$\frac{\partial \delta_3}{\partial Q_2}$	$\frac{\partial \delta_3}{\partial Q_3}$
$\frac{\partial \delta_4}{\partial \mathrm{P}_2}$	$\frac{\partial \delta_4}{\partial \mathrm{P}_3}$	$\frac{\partial \delta_4}{\partial \mathrm{P}_4}$	$\frac{\partial \delta_4}{\partial Q_2}$	$\frac{\partial \delta_4}{\partial Q_3}$
$\frac{\partial \lvert V_2 \rvert}{\partial P_2}$	$\frac{\partial \lvert V_2 \rvert}{\partial P_3}$	$\frac{\partial \lvert V_2 \rvert}{\partial P_4}$	$\frac{\partial \lvert V_2 \rvert}{\partial Q_2}$	$\frac{\partial \lvert V_2 \rvert}{\partial Q_3}$
$\frac{\partial \lvert V_3 \rvert}{\partial P_2}$	$\frac{\partial \lvert V_3 \rvert}{\partial P_3}$	$\frac{\partial \lvert V_3 \rvert}{\partial P_4}$	$\frac{\partial \lvert V_2 \rvert}{\partial Q_3}$	$\frac{\partial \lvert V_3 \rvert}{\partial Q_3}$

Values in the inverse of Jacobian matrix include PV bus elements are marked in Table 3. 3 and removed in Table 3. 4

Table 3. 3 Marking PV bus elements in the inverse Jacobian matrix of 4 buses

$\frac{\partial \delta_2}{\partial \mathrm{P}_2}$	$\frac{\partial \delta_2}{\partial \mathrm{P}_3}$	$\frac{\partial \delta_2}{\partial \mathrm{P}_4}$	$\frac{\partial \delta_2}{\partial Q_2}$	$\frac{\partial \delta_2}{\partial Q_3}$
$\frac{\partial \delta_3}{\partial \mathrm{P}_2}$	$\frac{\partial \delta_3}{\partial \mathrm{P}_3}$	$\frac{\partial \delta_3}{\partial \mathrm{P}_4}$	$\frac{\partial \delta_3}{\partial Q_2}$	$\frac{\partial \delta_3}{\partial Q_3}$
$\frac{\partial \delta_4}{\partial \mathrm{P}_2}$	$\frac{\partial \delta_4}{\partial \mathrm{P}_3}$	$\frac{\partial \delta_4}{\partial \mathrm{P}_4}$	$\frac{\partial \delta_4}{\partial Q_2}$	$\frac{\partial \delta_4}{\partial Q_3}$
$\frac{\partial \lvert V_2 \rvert}{\partial P_2}$	$\frac{\partial \lvert V_2 \rvert}{\partial P_3}$	$\frac{\partial \lvert V_2 \rvert}{\partial P_4}$	$\frac{\partial \lvert V_2 \rvert}{\partial Q_2}$	$\frac{\partial \lvert V_2 \rvert}{\partial Q_3}$
$\frac{\partial \lvert V_3 \rvert}{\partial P_2}$	$\frac{\partial \lvert V_3 \rvert}{\partial P_3}$	$\frac{\partial \lvert V_3 \rvert}{\partial P_4}$	$\frac{\partial \lvert V_2 \rvert}{\partial Q_3}$	$\frac{\partial \lvert V_3 \rvert}{\partial Q_3}$

Table 3. 4 removed PV bus elements in the inverse Jacobian matrix of 4 buses

$\frac{\partial \delta_2}{\partial \mathrm{P}_2}$	$\frac{\partial \delta_2}{\partial \mathrm{P}_3}$	$\frac{\partial \delta_2}{\partial Q_2}$	$\frac{\partial \delta_2}{\partial Q_3}$
$\frac{\partial \delta_3}{\partial \mathrm{P}_2}$	$\frac{\partial \delta_3}{\partial \mathrm{P}_3}$	$\frac{\partial \delta_3}{\partial Q_2}$	$\frac{\partial \delta_3}{\partial Q_3}$
$\frac{\partial \lvert V_2 \rvert}{\partial P_2}$	$\frac{\partial \lvert V_2 \rvert}{\partial P_3}$	$\frac{\partial \lvert V_2 \rvert}{\partial Q_2}$	$\frac{\partial \lvert V_2 \rvert}{\partial Q_3}$
$\frac{\partial \lvert V_3 \rvert}{\partial P_2}$	$\frac{\partial \lvert V_3 \rvert}{\partial P_3}$	$\frac{\partial \lvert V_2 \rvert}{\partial Q_3}$	$\frac{\partial \lvert V_3 \rvert}{\partial Q_3}$

Now the four sub-matrices of the inverse Jacobian matrix are all in the same size, PV bus elements are removed.

3. 4 The definition of indices

Four basic sensitivity indices have been proposed in [35]. Four basic indices are shown in equation (3. 31) – (3. 34), the indices are the summation of the columns of the inverse Jacobian matrix and divided by the number of PQ buses. The sensitivity of voltage angle and magnitude to the active and reactive power can be displayed as the mathematical weighted form.

$$\mathrm{Index}_{APi} = \frac{\sum_{k=1}^{n} \left| \frac{\partial \delta_k}{\partial P_i} \right|}{npq} \tag{3. 31}$$

$$\text{Index}_{VPi} = \frac{\sum_{k=1}^{n} \left| \frac{\partial |V_k|}{\partial P_i} \right|}{npq} \quad (3.\ 32)$$

$$\text{Index}_{AQi} = \frac{\sum_{k=1}^{n} \left| \frac{\partial \delta_k}{\partial Q_i} \right|}{npq} \quad (3.\ 33)$$

$$\text{Index}_{VQi} = \frac{\sum_{k=1}^{n} \left| \frac{\partial |V_k|}{\partial Q_i} \right|}{npq} \quad (3.\ 34)$$

Where i and npq are the number of PQ bus in the system. The summation of the columns of the inverse of Jacobian matrix meaning the sensitivity of the voltage angle and magnitude to the active and reactive power injection.

The high value means the large impact will make to the voltage angle and magnitude. It should be mentioned that nodes with higher sensitivity index value can influence voltage angle and magnitude at other nodes better, it is more effective to place a storage system at the node with the high sensitivity index value.

Index_{APi} describes the influence of injected active power at bus i on the collective angle improvement in all of the network. Index_{VPi} means the sensitivity of voltage magnitude to the active power injection. Index_{AQi} is the influence of injected reactive power at bus i on the collective angle and Index_{VQi} is the influence of the injected reactive power to the voltage magnitude.

Since voltage angle is more sensitive to the active power compared to the reactive power and the magnitude is more under the influence of the reactive power rather than the active

power, Index_{APi} and Index_{VQi} are dominant indices. The values of sensitivity indices in dominant indices are greater than the non-dominant indices which are Index_{AQi} and Index_{VPi}.

The following compound indices are defined to describe the system in more meaningful ways. Index_{APi} minus Index_{VPi} is defined as Index_{Pi}, which means how much active power can influences the angle but not the magnitude.

Index_{AQi} is subtracted from Index_{VQi} to obtain the influence of reactive power on the magnitude rather than the angle, Index_{Qi} and Index_{Ai} represents how much can the voltage angle be influenced by the active power injection but not reactive power. Similarly, Index_{Vi} shows how much the voltage magnitude can be influenced by the reactive power injection. The equations of four new defined indices are:

$$\text{Index}_{Pi} = \text{Index}_{APi} - \text{Index}_{VPi} \quad (3.35)$$

$$\text{Index}_{Qi} = \text{Index}_{VQi} - \text{Index}_{AQi} \quad (3.36)$$

$$\text{Index}_{Ai} = \text{Index}_{APi} - \text{Index}_{AQi} \quad (3.37)$$

$$\text{Index}_{Vi} = \text{Index}_{VQi} - \text{Index}_{VPi} \quad (3.38)$$

The summation of Index_{Pi} and Index_{Qi} is equal to the summation of Index_{Ai} and Index_{Vi} and it represents the mathematical weighted index to show how much the collective voltage angle and magnitude of a network can be influenced by the injected active and reactive powers.

$$\text{Index}_{Ti} = \text{Index}_{Pi} + \text{Index}_{Qi} \quad (3.\ 39)$$

The value of Index_{Ti} represent how much that voltage angle and magnitude will be influenced by the injection of apparent power S at bus *i*. The higher value means the voltage angle and magnitude at the rest of the bus will be influenced by the injection of apparent power S at bus *i* significantly.

3. 5 IEEE 14-node test feeder as a case study for sensitivity indices

To demonstrate how to apply the Newton-Raphson load flow and obtain the Jacobian matrix, the IEEE 14-node test feeder was chosen as an example. The test feeder includes 14 buses, 5 generators, and 11 loads. The system is shown in Figure 3.2.

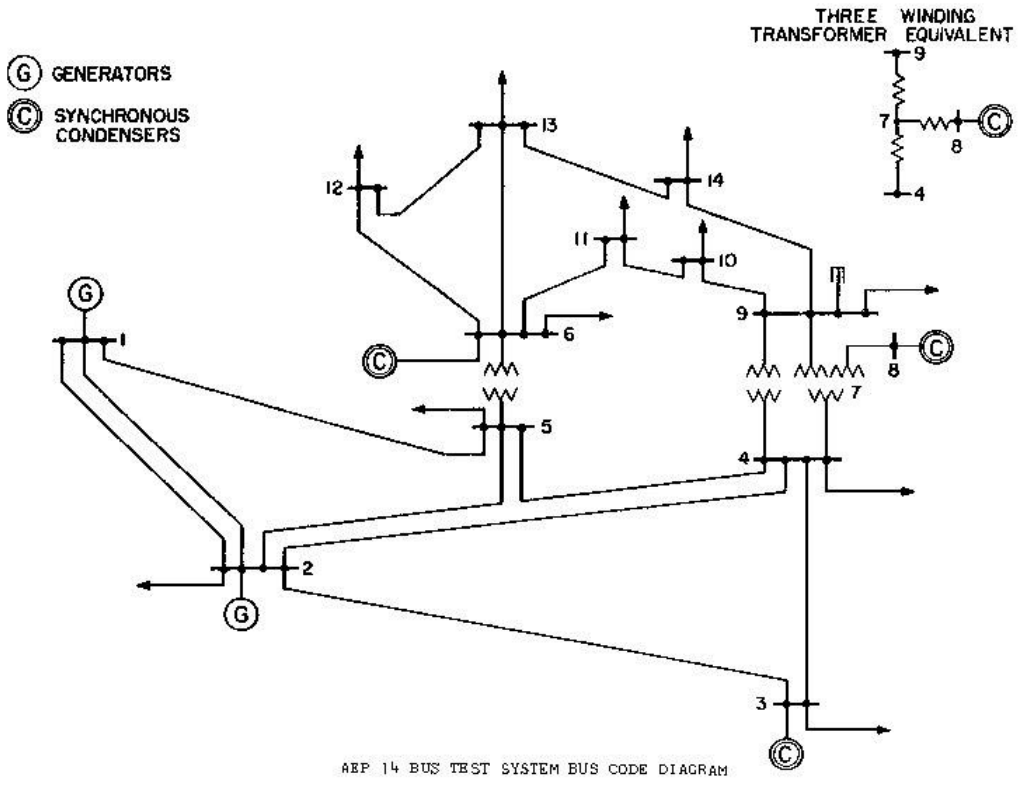

Figure 3.2 IEEE 14-node test feeder

The system, including one slack bus, four PV buses and nine PQ buses. The testing model is constructed in Matlab. After solving power flow with the Newton-Raphson method, the Jacobian matrix is obtained and shown in Table 3.5.

Table 3.5 Jacobian matrix obtained from IEEE 14 bus

32.706	-5.163	-5.557	-5.625	0.000	0.000	0.000	0.000	0.000	0.000	0.000	0.000	0.000	-1.265	-1.417	0.000	0.000	0.000	0.000	0.000	0.000	0.000
-4.839	9.932	-5.093	0.000	0.000	0.000	0.000	0.000	0.000	0.000	0.000	0.000	0.000	-2.228	0.000	0.000	0.000	0.000	0.000	0.000	0.000	0.000
-5.230	-5.271	39.642	-22.036	0.000	-5.173	0.000	-1.931	0.000	0.000	0.000	0.000	0.000	10.180	-7.494	0.259	0.150	0.000	0.000	0.000	0.000	0.000
-5.387	0.000	-22.400	36.737	-4.608	0.000	0.000	0.000	0.000	0.000	0.000	0.000	0.000	-6.385	9.652	0.000	0.000	0.000	0.000	0.000	0.000	0.000
0.000	0.000	0.000	-4.608	19.698	0.000	0.000	0.000	0.000	-4.598	-3.604	-6.887	0.000	0.000	-0.451	0.000	0.000	0.000	-2.060	-1.582	-3.215	0.000
0.000	0.000	-5.173	0.000	0.000	21.377	-6.411	-9.792	0.000	0.000	0.000	0.000	0.000	-0.267	0.000	0.000	0.263	0.000	0.000	0.000	0.000	0.000
0.000	0.000	0.000	0.000	0.000	-6.411	6.411	0.000	0.000	0.000	0.000	0.000	0.000	0.000	0.000	0.000	0.000	0.000	0.000	0.000	0.000	0.000
0.000	0.000	-1.931	0.000	0.000	-9.792	0.000	25.954	-11.017	0.000	0.000	0.000	-3.214	-0.153	0.000	-0.259	5.202	-3.981	0.000	0.000	0.000	-1.399
0.000	0.000	0.000	0.000	0.000	0.000	0.000	-10.986	15.723	-4.738	0.000	0.000	0.000	0.000	0.000	0.000	-4.059	5.869	-1.951	0.000	0.000	0.000
0.000	0.000	0.000	0.000	-4.567	0.000	0.000	0.000	-4.750	9.317	0.000	0.000	0.000	0.000	0.000	0.000	0.000	-1.953	3.979	0.000	0.000	0.000
0.000	0.000	0.000	0.000	-3.553	0.000	0.000	0.000	0.000	0.000	6.038	-2.484	0.000	0.000	0.000	0.000	0.000	0.000	0.000	4.171	-2.620	0.000
0.000	0.000	0.000	0.000	-6.780	0.000	0.000	0.000	0.000	0.000	-2.481	11.746	-2.485	0.000	0.000	0.000	0.000	0.000	0.000	-2.607	6.910	-1.159
0.000	0.000	0.000	0.000	0.000	0.000	0.000	-3.148	0.000	0.000	0.000	-2.454	5.602	0.000	0.000	0.000	-1.519	0.000	0.000	0.000	-1.189	2.464
2.274	1.803	-11.270	7.619	0.000	-0.271	0.000	-0.155	0.000	0.000	0.000	0.000	0.000	39.203	-21.677	-4.947	-1.874	0.000	0.000	0.000	0.000	0.000
2.166	0.000	6.469	-9.964	-0.459	0.000	0.000	0.000	0.000	0.000	0.000	0.000	0.000	-22.109	36.107	0.000	0.000	0.000	0.000	0.000	0.000	0.000
0.000	0.000	0.271	0.000	0.000	0.000	0.000	-0.271	0.000	0.000	0.000	0.000	0.000	-5.106	0.000	20.442	-9.502	0.000	0.000	0.000	0.000	0.000
0.000	0.000	0.155	0.000	0.000	0.271	0.000	-5.951	4.100	0.000	0.000	0.000	1.426	-1.906	0.000	-9.364	24.863	-10.697	0.000	0.000	0.000	-3.153
0.000	0.000	0.000	0.000	0.000	0.000	0.000	4.183	-6.224	2.041	0.000	0.000	0.000	0.000	0.000	0.000	-10.660	15.154	-4.529	0.000	0.000	0.000
0.000	0.000	0.000	0.000	2.221	0.000	0.000	0.000	2.012	-4.233	0.000	0.000	0.000	0.000	0.000	0.000	0.000	-4.612	8.872	0.000	0.000	0.000
0.000	0.000	0.000	0.000	1.773	0.000	0.000	0.000	0.000	0.000	-4.515	2.742	0.000	0.000	0.000	0.000	0.000	0.000	0.000	5.702	-2.373	0.000
0.000	0.000	0.000	0.000	3.576	0.000	0.000	0.000	0.000	0.000	2.745	-7.502	1.181	0.000	0.000	0.000	0.000	0.000	0.000	-2.355	11.112	-2.438
0.000	0.000	0.000	0.000	0.000	0.000	0.000	1.565	0.000	0.000	0.000	1.245	-2.810	0.000	0.000	0.000	-3.055	0.000	0.000	0.000	-2.344	5.398

The size of the Jacobian matrix can be calculated in (3.24), the number of PV bus is four, PQ bus is nine and one slack bus.

$$J_{(npv+2\times npq)\times(npv+2\times npq)} \tag{3. 24}$$

Where *npv* is four and *npq* is nine, the size of Jacobian matrix is $J_{(22)\times(22)}$. Then inverse the Jacobian matrix and get inverse Jacobian matrix shows in Table 3.6. Matlab software is used to implement the method. Gray boxes show the corresponding code in the text throughout this thesis.

```
Jinv = abs(100*inv(J));
```

Where Jinv is the inverse of Jacobian matrix. Since the numerical values of Jinv are small, it is multiplied by 100 for the sake of presentation. The absolute value of Jinv is considered so that negative and positive values do not cancel out each other. Table 3.6 shows Jinv that are generated from the above codes.

Table 3.6 Inverse Jacobian matrix of IEEE 14-node test feeder

5.097	4.918	4.312	3.894	4.017	4.261	4.261	4.232	4.219	4.132	4.093	4.127	4.277	0.110	0.170	0.053	0.061	0.066	0.041	0.024	0.042	0.085
4.556	16.347	7.541	6.072	6.522	7.353	7.353	7.244	7.159	6.866	6.671	6.755	7.184	0.505	0.506	0.202	0.181	0.174	0.098	0.051	0.079	0.189
4.038	7.503	9.880	7.700	8.343	9.427	9.427	9.201	9.090	8.742	8.533	8.621	9.121	0.888	0.278	0.423	0.436	0.331	0.153	0.017	0.007	0.181
3.677	6.088	7.705	8.844	8.421	7.866	7.866	7.964	8.091	8.280	8.517	8.517	8.380	0.485	0.807	0.131	0.038	0.007	0.025	0.027	0.067	0.075
3.792	6.556	8.619	8.690	23.608	12.506	12.506	14.610	16.348	20.028	23.326	22.798	18.652	0.059	0.125	0.864	1.752	1.603	0.913	0.102	0.467	1.400
3.977	7.268	9.575	7.953	12.164	21.846	21.846	18.111	17.126	14.702	12.772	13.241	16.282	0.655	0.224	0.440	0.850	0.687	0.353	0.073	0.031	0.407
3.977	7.268	9.575	7.953	12.164	21.846	37.443	18.111	17.126	14.702	12.772	13.241	16.282	0.655	0.224	0.440	0.850	0.687	0.353	0.073	0.031	0.407
3.945	7.143	9.391	8.070	14.132	18.190	18.190	22.833	21.379	17.831	14.963	15.643	20.064	0.597	0.235	0.352	0.826	0.675	0.358	0.121	0.016	0.374
3.918	7.038	9.252	8.180	15.825	17.172	17.172	21.359	27.001	21.492	16.456	16.920	19.808	0.504	0.217	0.146	0.388	2.791	1.451	0.116	0.067	0.071
3.855	6.797	8.931	8.430	19.692	14.841	14.841	17.988	21.670	29.659	19.869	19.836	19.218	0.298	0.181	0.309	0.582	0.757	4.351	0.102	0.253	0.600
3.803	6.597	8.683	8.653	22.960	12.915	12.915	15.201	16.719	19.892	35.651	26.578	20.669	0.072	0.118	0.855	1.723	1.569	0.888	7.874	0.764	0.870
3.813	6.637	8.725	8.604	22.296	13.291	13.291	15.745	17.042	19.722	26.428	29.749	22.353	0.136	0.142	0.688	1.379	1.275	0.731	1.116	3.799	0.649
3.888	6.924	9.116	8.312	17.702	16.079	16.079	19.777	19.523	18.680	20.010	21.915	35.671	0.359	0.171	0.215	0.363	0.364	0.212	0.327	1.499	6.920
0.008	0.156	1.669	1.008	1.279	1.974	1.974	2.070	1.972	1.648	1.344	1.442	1.888	4.043	2.520	1.750	1.673	1.386	0.699	0.133	0.247	1.073
0.038	0.219	1.229	1.555	1.671	1.594	1.594	1.749	1.766	1.734	1.695	1.731	1.814	2.493	4.128	1.119	1.110	0.926	0.472	0.086	0.172	0.723
0.011	0.099	0.797	0.428	0.119	1.471	1.471	1.927	1.716	0.974	0.212	0.458	1.488	1.812	1.141	7.825	5.414	4.474	2.252	0.404	0.768	3.428
0.022	0.141	0.831	0.369	0.597	1.854	1.854	2.645	2.282	0.951	0.448	0.012	1.875	1.718	1.099	5.368	10.760	8.891	4.475	0.796	1.521	6.803
0.020	0.123	0.699	0.300	0.597	1.603	1.603	2.288	4.632	2.195	0.462	0.066	1.575	1.423	0.913	4.452	8.924	14.156	7.122	0.662	1.260	5.641
0.012	0.070	0.369	0.148	0.414	0.890	0.890	1.271	2.531	5.404	0.332	0.115	0.827	0.727	0.469	2.279	4.566	7.230	12.998	0.341	0.643	2.885
0.000	0.005	0.055	0.033	0.040	0.087	0.087	0.122	0.124	0.090	8.826	1.578	0.864	0.132	0.082	0.407	0.817	0.677	0.342	13.749	4.682	2.569
0.005	0.027	0.133	0.049	0.186	0.336	0.336	0.481	0.394	0.120	1.341	4.632	2.514	0.252	0.164	0.793	1.588	1.311	0.658	4.663	8.661	4.811
0.015	0.094	0.538	0.233	0.443	1.226	1.226	1.750	1.497	0.596	0.312	2.030	9.749	1.099	0.704	3.437	6.890	5.692	2.864	2.527	4.722	21.122

In the system, there are four PV buses. PV buses are already connected to a local generator or utility and hence they do not need a storage device to help the angle or voltage profile. Nodes with PV buses need to be removed from the inverse Jacobian matrix. To do that, J_1^{-1}, J_2^{-1}, J_3^{-1}, and J_4^{-1} have to be identified from the matrix.

From equation (3.25) – (3.28), the size of four sub-matrices can be calculated. After the processing, J_1^{-1}, J_2^{-1}, J_3^{-1}, and J_4^{-1} can be identified and shown in Table 3.7.

Table 3.7 The four groups of inverse Jacobian matrix

5.097	4.918	4.312	3.894	4.017	4.261	4.261	4.232	4.219	4.132	4.093	4.127	4.277	0.110	0.170	0.053	0.061	0.066	0.041	0.024	0.042	0.085
4.556	16.347	7.541	6.072	6.522	7.353	7.353	7.244	7.159	6.866	6.671	6.755	7.184	0.505	0.506	0.202	0.181	0.174	0.098	0.051	0.079	0.189
4.038	7.503	9.880	7.700	8.343	9.427	9.427	9.201	9.090	8.742	8.533	8.621	9.121	0.888	0.278	0.423	0.436	0.331	0.153	0.017	0.007	0.181
3.677	6.088	7.705	8.844	8.421	7.866	7.866	7.964	8.091	8.280	8.517	8.517	8.380	0.485	0.807	0.131	0.038	0.007	0.025	0.027	0.067	0.075
3.792	6.556	8.619	8.690	23.608	12.506	12.506	14.610	16.348	20.028	23.326	22.798	18.652	0.059	0.125	0.864	1.752	1.603	0.913	0.102	0.467	1.400
3.977	7.268	9.575	7.953	12.164	21.846	21.846	18.111	17.126	14.702	12.772	13.241	16.282	0.655	0.224	0.440	0.850	0.687	0.353	0.073	0.031	0.407
3.977	7.268	9.575	7.953	12.164	21.846	37.443	18.111	17.126	14.702	12.772	13.241	16.282	0.655	0.224	0.440	0.850	0.687	0.353	0.073	0.031	0.407
3.945	7.143	9.391	8.070	14.132	18.190	18.190	22.833	21.379	17.831	14.963	15.643	20.064	0.597	0.235	0.352	0.826	0.675	0.358	0.121	0.016	0.374
3.918	7.038	9.252	8.180	15.825	17.172	17.172	21.359	27.001	21.492	16.456	16.920	19.808	0.504	0.217	0.146	0.388	2.791	1.451	0.116	0.067	0.071
3.855	6.797	8.931	8.430	19.692	14.841	14.841	17.988	21.670	29.659	19.869	19.836	19.218	0.298	0.181	0.309	0.582	0.757	4.351	0.102	0.253	0.600
3.803	6.597	8.683	8.653	22.960	12.915	12.915	15.201	16.719	19.892	35.651	26.578	20.669	0.072	0.118	0.855	1.723	1.569	0.888	7.874	0.764	0.870
3.813	6.637	8.725	8.604	22.296	13.291	13.291	15.745	17.042	19.722	26.428	29.749	22.353	0.136	0.142	0.688	1.379	1.275	0.731	1.116	3.799	0.649
3.888	6.924	9.116	8.312	17.702	16.079	16.079	19.777	19.523	18.680	20.010	21.915	35.671	0.359	0.171	0.215	0.363	0.364	0.212	0.327	1.499	6.920
0.008	0.156	1.669	1.008	1.279	1.974	1.974	2.070	1.972	1.648	1.344	1.442	1.888	4.043	2.520	1.750	1.673	1.386	0.699	0.133	0.247	1.073
0.038	0.219	1.229	1.555	1.671	1.594	1.594	1.749	1.766	1.734	1.695	1.731	1.814	2.493	4.128	1.119	1.110	0.926	0.472	0.086	0.172	0.723
0.011	0.099	0.797	0.428	0.119	1.471	1.471	1.927	1.716	0.974	0.212	0.458	1.488	1.812	1.141	7.825	5.414	4.474	2.252	0.404	0.768	3.428
0.022	0.141	0.831	0.369	0.597	1.854	1.854	2.645	2.282	0.951	0.448	0.012	1.875	1.718	1.099	5.368	10.760	8.891	4.475	0.796	1.521	6.803
0.020	0.123	0.699	0.300	0.597	1.603	1.603	2.288	4.632	2.195	0.462	0.066	1.575	1.423	0.913	4.452	8.924	14.156	7.122	0.662	1.260	5.641
0.012	0.070	0.369	0.148	0.414	0.890	0.890	1.271	2.531	5.404	0.332	0.115	0.827	0.727	0.469	2.279	4.566	7.230	12.998	0.341	0.643	2.885
0.000	0.005	0.055	0.033	0.040	0.087	0.087	0.122	0.124	0.090	8.826	1.578	0.864	0.132	0.082	0.407	0.817	0.677	0.342	13.749	4.682	2.569
0.005	0.027	0.133	0.049	0.186	0.336	0.336	0.481	0.394	0.120	1.341	4.632	2.514	0.252	0.164	0.793	1.588	1.311	0.658	4.663	8.661	4.811
0.015	0.094	0.538	0.233	0.443	1.226	1.226	1.750	1.497	0.596	0.312	2.030	9.749	1.099	0.704	3.437	6.890	5.692	2.864	2.527	4.722	21.122

Once the four sub-matrices of the inverse of Jacobian matrix are identified, the PV bus elements can be identified and removed. The following code identifies values that contain PV bus elements, the sub-matrix J_1^{-1} contain PV bus elements in both column and row as it is shown in Table 3.8. In the following code, type is number in one of the three types of nodes, slack bus is set as type 1, PV is type 2 and PQ is type 3.

Table 3.8 PV bus elements in J_1^{-1}matrix

5.097	4.918	4.312	3.894	4.017	4.261	4.261	4.232	4.219	4.132	4.093	4.127	4.277
4.556	16.347	7.541	6.072	6.522	7.353	7.353	7.244	7.159	6.866	6.671	6.755	7.184
4.038	7.503	9.880	7.700	8.343	9.427	9.427	9.201	9.090	8.742	8.533	8.621	9.121
3.677	6.088	7.705	8.844	8.421	7.866	7.866	7.964	8.091	8.280	8.517	8.517	8.380
3.792	6.556	8.619	8.690	23.608	12.506	12.506	14.610	16.348	20.028	23.326	22.798	18.652
3.977	7.268	9.575	7.953	12.164	21.846	21.846	18.111	17.126	14.702	12.772	13.241	16.282
3.977	7.268	9.575	7.953	12.164	21.846	37.443	18.111	17.126	14.702	12.772	13.241	16.282
3.945	7.143	9.391	8.070	14.132	18.190	18.190	22.833	21.379	17.831	14.963	15.643	20.064
3.918	7.038	9.252	8.180	15.825	17.172	17.172	21.359	27.001	21.492	16.456	16.920	19.808
3.855	6.797	8.931	8.430	19.692	14.841	14.841	17.988	21.670	29.659	19.869	19.836	19.218
3.803	6.597	8.683	8.653	22.960	12.915	12.915	15.201	16.719	19.892	35.651	26.578	20.669
3.813	6.637	8.725	8.604	22.296	13.291	13.291	15.745	17.042	19.722	26.428	29.749	22.353
3.888	6.924	9.116	8.312	17.702	16.079	16.079	19.777	19.523	18.680	20.010	21.915	35.671

```
Jinv1=zeros(npq+npv,npq+npv);
for i=1:nbus-1
    for j=1:nbus-1
    if type(i+1)==3 && type(j+1)==3
        Jinv1(j,i)=Jinv(j,i)
    end
end
end
```

After identifying and removing all of the columns and rows that contain PV bus elements, the program finds the new J_1^{-1} matrix and it has shown in Table 3.9.

```
npv=npv-1;
Jinv1(find(Jinv1==0))=[];
Jinv1=reshape(Jinv1,npq,npq);
```

Table 3.9 New J_1^{-1} matrix

9.880	7.700	9.427	9.201	9.090	8.742	8.533	8.621	9.121
7.705	8.844	7.866	7.964	8.091	8.280	8.517	8.517	8.380
9.575	7.953	21.846	18.111	17.126	14.702	12.772	13.241	16.282
9.391	8.070	18.190	22.833	21.379	17.831	14.963	15.643	20.064
9.252	8.180	17.172	21.359	27.001	21.492	16.456	16.920	19.808
8.931	8.430	14.841	17.988	21.670	29.659	19.869	19.836	19.218
8.683	8.653	12.915	15.201	16.719	19.892	35.651	26.578	20.669
8.725	8.604	13.291	15.745	17.042	19.722	26.428	29.749	22.353
9.116	8.312	16.079	19.777	19.523	18.680	20.010	21.915	35.671

In the sub-matrix J_2^{-1}, only PV rows exist. The process that finding PV bus elements in matrix is shown below and results are shown in Table 3.10.

```
Jinv2=zeros(npq+npv,npq);
for i=npq+npv+1:npq+npv+npq
    for j=1:npq+npv
    if type(j+1)==3
        Jinv2(j,i-npq-npv)=Jinv(j,i)
    end
end
end
```

Table 3.10 PV bus element in J_2^{-1} matrix

0.110	0.170	0.053	0.061	0.066	0.041	0.024	0.042	0.085
0.505	0.506	0.202	0.181	0.174	0.098	0.051	0.079	0.189
0.888	0.278	0.423	0.436	0.331	0.153	0.017	0.007	0.181
0.485	0.807	0.131	0.038	0.007	0.025	0.027	0.067	0.075
0.059	0.125	0.864	1.752	1.603	0.913	0.102	0.467	1.400
0.655	0.224	0.440	0.850	0.687	0.353	0.073	0.031	0.407
0.655	0.224	0.440	0.850	0.687	0.353	0.073	0.031	0.407
0.597	0.235	0.352	0.826	0.675	0.358	0.121	0.016	0.374
0.504	0.217	0.146	0.388	2.791	1.451	0.116	0.067	0.071
0.298	0.181	0.309	0.582	0.757	4.351	0.102	0.253	0.600
0.072	0.118	0.855	1.723	1.569	0.888	7.874	0.764	0.870
0.136	0.142	0.688	1.379	1.275	0.731	1.116	3.799	0.649
0.359	0.171	0.215	0.363	0.364	0.212	0.327	1.499	6.920

The new J_2^{-1} matrix has shown in Table 3.11. The size of the sub-matrix now becomes 9×9. The red blocks in Table 3.10 have been removed.

```
Jinv2(find(Jinv2==0))=[];
Jinv2=reshape(Jinv2,npq,npq);
```

Table 3.11 New J_2^{-1}matrix

1.669	1.008	1.974	2.070	1.972	1.648	1.344	1.442	1.888
1.229	1.555	1.594	1.749	1.766	1.734	1.695	1.731	1.814
0.797	0.428	1.471	1.927	1.716	0.974	0.212	0.458	1.488
0.831	0.369	1.854	2.645	2.282	0.951	0.448	0.012	1.875
0.699	0.300	1.603	2.288	4.632	2.195	0.462	0.066	1.575
0.369	0.148	0.890	1.271	2.531	5.404	0.332	0.115	0.827
0.055	0.033	0.087	0.122	0.124	0.090	8.826	1.578	0.864
0.133	0.049	0.336	0.481	0.394	0.120	1.341	4.632	2.514
0.538	0.233	1.226	1.750	1.497	0.596	0.312	2.030	9.749

In J_3^{-1} matrix, PV bus elements need to be removed in columns. The result of identifying PV bus elements shown in Table 3. 11 as red blocks.

```
Jinv3=zeros(npq,npq+npv);
for i=1:npq+npv
    for j=npq+npv+1:npq+npv+npq
    if  type(i+1)==3
        Jinv3(j-npq-npv,i)=Jinv(j,i)
    end
end
end
```

Table 3.12 PV bus element identified in J_3^{-1}

0.008	0.156	1.669	1.008	1.279	1.974	1.974	2.070	1.972	1.648	1.344	1.442	1.888
0.038	0.219	1.229	1.555	1.671	1.594	1.594	1.749	1.766	1.734	1.695	1.731	1.814
0.011	0.099	0.797	0.428	0.119	1.471	1.471	1.927	1.716	0.974	0.212	0.458	1.488
0.022	0.141	0.831	0.369	0.597	1.854	1.854	2.645	2.282	0.951	0.448	0.012	1.875
0.020	0.123	0.699	0.300	0.597	1.603	1.603	2.288	4.632	2.195	0.462	0.066	1.575
0.012	0.070	0.369	0.148	0.414	0.890	0.890	1.271	2.531	5.404	0.332	0.115	0.827
0.000	0.005	0.055	0.033	0.040	0.087	0.087	0.122	0.124	0.090	8.826	1.578	0.864
0.005	0.027	0.133	0.049	0.186	0.336	0.336	0.481	0.394	0.120	1.341	4.632	2.514
0.015	0.094	0.538	0.233	0.443	1.226	1.226	1.750	1.497	0.596	0.312	2.030	9.749

New J_3^{-1} matrix after removing PV bus elements has been shown in Table 3.13.

```
Jinv3(find(Jinv3==0))=[];
Jinv3=reshape(Jinv3,npq,npq);
```

Table 3.13 The new J_3^{-1} matrix

1.669	1.008	1.974	2.070	1.972	1.648	1.344	1.442	1.888
1.229	1.555	1.594	1.749	1.766	1.734	1.695	1.731	1.814
0.797	0.428	1.471	1.927	1.716	0.974	0.212	0.458	1.488
0.831	0.369	1.854	2.645	2.282	0.951	0.448	0.012	1.875
0.699	0.300	1.603	2.288	4.632	2.195	0.462	0.066	1.575
0.369	0.148	0.890	1.271	2.531	5.404	0.332	0.115	0.827
0.055	0.033	0.087	0.122	0.124	0.090	8.826	1.578	0.864
0.133	0.049	0.336	0.481	0.394	0.120	1.341	4.632	2.514
0.538	0.233	1.226	1.750	1.497	0.596	0.312	2.030	9.749

In J_4^{-1} matrix, only PQ bus elements existing, no change need to be done in J_4^{-1}. Table 3.14 shows the J_4^{-1} matrix.

```
Jinv4=zeros(npq,npq);
for i=npq+npv+1:npq+npv+npq
    for j=npq+npv+1:npq+npv+npq
        Jinv4(j-npq-npv,i-npv-npq)=Jinv(j,i)
    end
end
```

Table 3.14 J_4^{-1} matrix

4.043	2.520	1.750	1.673	1.386	0.699	0.133	0.247	1.073
2.493	4.128	1.119	1.110	0.926	0.472	0.086	0.172	0.723
1.812	1.141	7.825	5.414	4.474	2.252	0.404	0.768	3.428
1.718	1.099	5.368	10.760	8.891	4.475	0.796	1.521	6.803
1.423	0.913	4.452	8.924	14.156	7.122	0.662	1.260	5.641
0.727	0.469	2.279	4.566	7.230	12.998	0.341	0.643	2.885
0.132	0.082	0.407	0.817	0.677	0.342	13.749	4.682	2.569
0.252	0.164	0.793	1.588	1.311	0.658	4.663	8.661	4.811
1.099	0.704	3.437	6.890	5.692	2.864	2.527	4.722	21.122

The process that identifies and removes PV bus elements in the whole matrix is shown in Table 3. 15 and Table 3. 16. The red blocks in Table 3. 15 are values that contain PV bus elements.

Table 3. 15 identified PV bus element

5.097	4.918	4.312	3.894	4.017	4.261	4.261	4.232	4.219	4.132	4.093	4.127	4.277	0.110	0.170	0.053	0.061	0.066	0.041	0.024	0.042	0.085
4.556	16.347	7.541	6.072	6.522	7.353	7.353	7.244	7.159	6.866	6.671	6.755	7.184	0.505	0.506	0.202	0.181	0.174	0.098	0.051	0.079	0.189
4.038	7.503	9.880	7.700	8.343	9.427	9.427	9.201	9.090	8.742	8.533	8.621	9.121	0.888	0.278	0.423	0.436	0.331	0.153	0.017	0.007	0.181
3.677	6.088	7.705	8.844	8.421	7.866	7.866	7.964	8.091	8.280	8.517	8.517	8.380	0.485	0.807	0.131	0.038	0.007	0.025	0.027	0.067	0.075
3.792	6.556	8.619	8.690	23.608	12.506	12.506	14.610	16.348	20.028	23.326	22.798	18.652	0.059	0.125	0.864	1.752	1.603	0.913	0.102	0.467	1.400
3.977	7.268	9.575	7.953	12.164	21.846	21.846	18.111	17.126	14.702	12.772	13.241	16.282	0.655	0.224	0.440	0.850	0.687	0.353	0.073	0.031	0.407
3.977	7.268	9.575	7.953	12.164	21.846	37.443	18.111	17.126	14.702	12.772	13.241	16.282	0.655	0.224	0.440	0.850	0.687	0.353	0.073	0.031	0.407
3.945	7.143	9.391	8.070	14.132	18.190	18.190	22.833	21.379	17.831	14.963	15.643	20.064	0.597	0.235	0.352	0.826	0.675	0.358	0.121	0.016	0.374
3.918	7.038	9.252	8.180	15.825	17.172	17.172	21.359	27.001	21.492	16.456	16.920	19.808	0.504	0.217	0.146	0.388	2.791	1.451	0.116	0.067	0.071
3.855	6.797	8.931	8.430	19.692	14.841	14.841	17.988	21.670	29.659	19.869	19.836	19.218	0.298	0.181	0.309	0.582	0.757	4.351	0.102	0.253	0.600
3.803	6.597	8.683	8.653	22.960	12.915	12.915	15.201	16.719	19.892	35.651	26.578	20.669	0.072	0.118	0.855	1.723	1.569	0.888	7.874	0.764	0.870
3.813	6.637	8.725	8.604	22.296	13.291	13.291	15.745	17.042	19.722	26.428	29.749	22.353	0.136	0.142	0.688	1.379	1.275	0.731	1.116	3.799	0.649
3.888	6.924	9.116	8.312	17.702	16.079	16.079	19.777	19.523	18.680	20.010	21.915	35.671	0.359	0.171	0.215	0.363	0.364	0.212	0.327	1.499	6.920
0.008	0.156	1.669	1.008	1.279	1.974	1.974	2.070	1.972	1.648	1.344	1.442	1.888	4.043	2.520	1.750	1.673	1.386	0.699	0.133	0.247	1.073
0.038	0.219	1.229	1.555	1.671	1.594	1.594	1.749	1.766	1.734	1.695	1.731	1.814	2.493	4.128	1.119	1.110	0.926	0.472	0.086	0.172	0.723
0.011	0.099	0.797	0.428	0.119	1.471	1.471	1.927	1.716	0.974	0.212	0.458	1.488	1.812	1.141	7.825	5.414	4.474	2.252	0.404	0.768	3.428
0.022	0.141	0.831	0.369	0.597	1.854	1.854	2.645	2.282	0.951	0.448	0.012	1.875	1.718	1.099	5.368	10.760	8.891	4.475	0.796	1.521	6.803
0.020	0.123	0.699	0.300	0.597	1.603	1.603	2.288	4.632	2.195	0.462	0.066	1.575	1.423	0.913	4.452	8.924	14.156	7.122	0.662	1.260	5.641
0.012	0.070	0.369	0.148	0.414	0.890	0.890	1.271	2.531	5.404	0.332	0.115	0.827	0.727	0.469	2.279	4.566	7.230	12.998	0.341	0.643	2.885
0.000	0.005	0.055	0.033	0.040	0.087	0.087	0.122	0.124	0.090	8.826	1.578	0.864	0.132	0.082	0.407	0.817	0.677	0.342	13.749	4.682	2.569
0.005	0.027	0.133	0.049	0.186	0.336	0.336	0.481	0.394	0.120	1.341	4.632	2.514	0.252	0.164	0.793	1.588	1.311	0.658	4.663	8.661	4.811
0.015	0.094	0.538	0.233	0.443	1.226	1.226	1.750	1.497	0.596	0.312	2.030	9.749	1.099	0.704	3.437	6.890	5.692	2.864	2.527	4.722	21.122

Table 3. 16 PV bus element are removed

9.880	7.700	9.427	9.201	9.090	8.742	8.533	8.621	9.121	0.888	0.278	0.423	0.436	0.331	0.153	0.017	0.007	0.181
7.705	8.844	7.866	7.964	8.091	8.280	8.517	8.517	8.380	0.485	0.807	0.131	0.038	0.007	0.025	0.027	0.067	0.075
9.575	7.953	21.846	18.111	17.126	14.702	12.772	13.241	16.282	0.655	0.224	0.440	0.850	0.687	0.353	0.073	0.031	0.407
9.391	8.070	18.190	22.833	21.379	17.831	14.963	15.643	20.064	0.597	0.235	0.352	0.826	0.675	0.358	0.121	0.016	0.374
9.252	8.180	17.172	21.359	27.001	21.492	16.456	16.920	19.808	0.504	0.217	0.146	0.388	2.791	1.451	0.116	0.067	0.071
8.931	8.430	14.841	17.988	21.670	29.659	19.869	19.836	19.218	0.298	0.181	0.309	0.582	0.757	4.351	0.102	0.253	0.600
8.683	8.653	12.915	15.201	16.719	19.892	35.651	26.578	20.669	0.072	0.118	0.855	1.723	1.569	0.888	7.874	0.764	0.870
8.725	8.604	13.291	15.745	17.042	19.722	26.428	29.749	22.353	0.136	0.142	0.688	1.379	1.275	0.731	1.116	3.799	0.649
9.116	8.312	16.079	19.777	19.523	18.680	20.010	21.915	35.671	0.359	0.171	0.215	0.363	0.364	0.212	0.327	1.499	6.920
1.669	1.008	1.974	2.070	1.972	1.648	1.344	1.442	1.888	4.043	2.520	1.750	1.673	1.386	0.699	0.133	0.247	1.073
1.229	1.555	1.594	1.749	1.766	1.734	1.695	1.731	1.814	2.493	4.128	1.119	1.110	0.926	0.472	0.086	0.172	0.723
0.797	0.428	1.471	1.927	1.716	0.974	0.212	0.458	1.488	1.812	1.141	7.825	5.414	4.474	2.252	0.404	0.768	3.428
0.831	0.369	1.854	2.645	2.282	0.951	0.448	0.012	1.875	1.718	1.099	5.368	10.760	8.891	4.475	0.796	1.521	6.803
0.699	0.300	1.603	2.288	4.632	2.195	0.462	0.066	1.575	1.423	0.913	4.452	8.924	14.156	7.122	0.662	1.260	5.641
0.369	0.148	0.890	1.271	2.531	5.404	0.332	0.115	0.827	0.727	0.469	2.279	4.566	7.230	12.998	0.341	0.643	2.885
0.055	0.033	0.087	0.122	0.124	0.090	8.826	1.578	0.864	0.132	0.082	0.407	0.817	0.677	0.342	13.749	4.682	2.569
0.133	0.049	0.336	0.481	0.394	0.120	1.341	4.632	2.514	0.252	0.164	0.793	1.588	1.311	0.658	4.663	8.661	4.811
0.538	0.233	1.226	1.750	1.497	0.596	0.312	2.030	9.749	1.099	0.704	3.437	6.890	5.692	2.864	2.527	4.722	21.122

The inverse of Jacobian matrix now is a group of four equal size sub-matrices. The indices for sensitivity analysis can be calculated. The indices from equation (3.28) – (3.31) can be obtained through the following code.

Index$_{AP}$ is the summation of columns in J_1^{-1} matrix and divide by the number of PQ bus (*npq*).

```
IndexAP=zeros(npq,1);
for i=1:npq
    for j=1:npq
    IndexAP(i)=IndexAP(i)+Jinv(j,i);
    end
end
IndexAP=IndexAP/npq;
```

IndexVP is the summation of columns in J_2^{-1} matrix and divide by the number of PQ bus.

```
IndexVP=zeros(npq,1);
for i=1:npq
    for j=npq+1:npq*2
        IndexVP(i)=IndexVP(i)+Jinv(j,i);
    end
end
IndexVP=IndexVP/npq;
```

IndexAQ is the summation of columns in J_3^{-1} matrix and divide by the number of PQ bus.

```
IndexAQ=zeros(npq,1);
```

```
for i=npq+1:npq*2
    for j=1:npq
    IndexAQ(i-npq)=IndexAQ(i-npq)+Jinv(j,i);
    end
end
IndexAQ=IndexAQ/npq;
```

IndexVQ is the summation of columns in J_4^{-1} matrix and divide by the number of PQ bus.

```
IndexVQ=zeros(npq,1);
for j=npq+1:npq*2
    for i=npq+1:npq*2
    IndexVQ(j-npq)=IndexVQ(j-npq)+Jinv(i,j);
    end
end
IndexVQ=IndexVQ/npq;
```

The five compound indices can be calculated from the four basic indices with equations (3. 35) - (3. 38).

```
IndexP=IndexAP-IndexVP;
IndexQ=IndexVQ-IndexAQ;
IndexA=IndexAP+IndexAQ;
IndexV=IndexVP+IndexVQ;
IndexT=IndexAP-IndexVP+IndexVQ-IndexAQ;
```

All four basic indices are calculated, and the results are shown in Figure 3. 3 – Figure 3. 6. The Y axis represents the mathematical weigh in percentage, all indices are on the same scale. The X axis is the node's number.

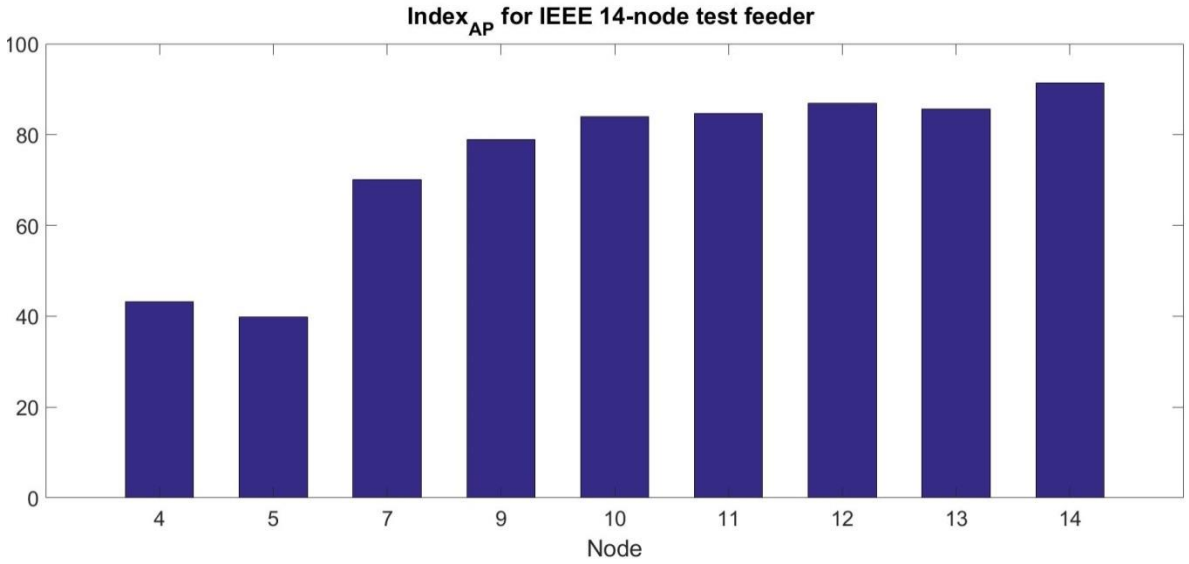

Figure 3. 3 Index_{AP} of 14-node system

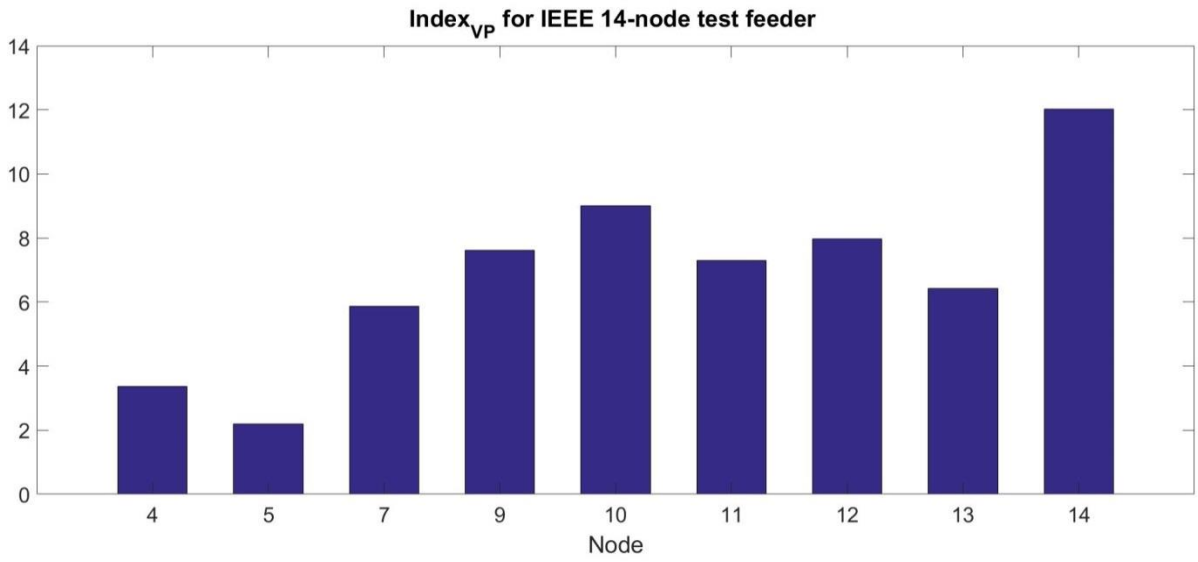

Figure 3. 4 Index_{VP} of 14-node system

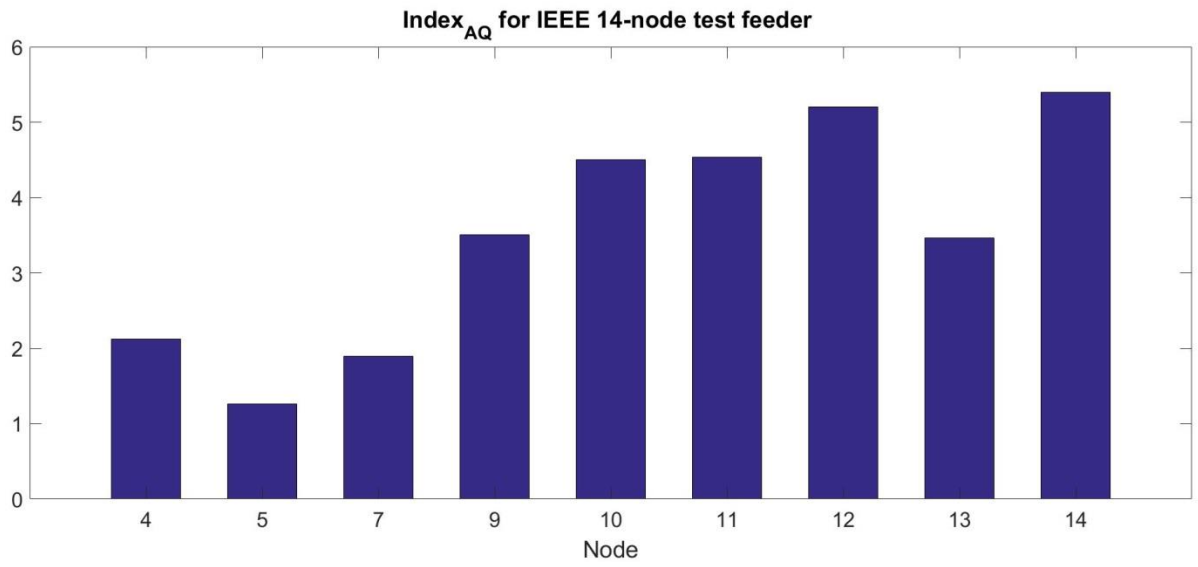

Figure 3. 5 Index_{AQ} of 14-node system

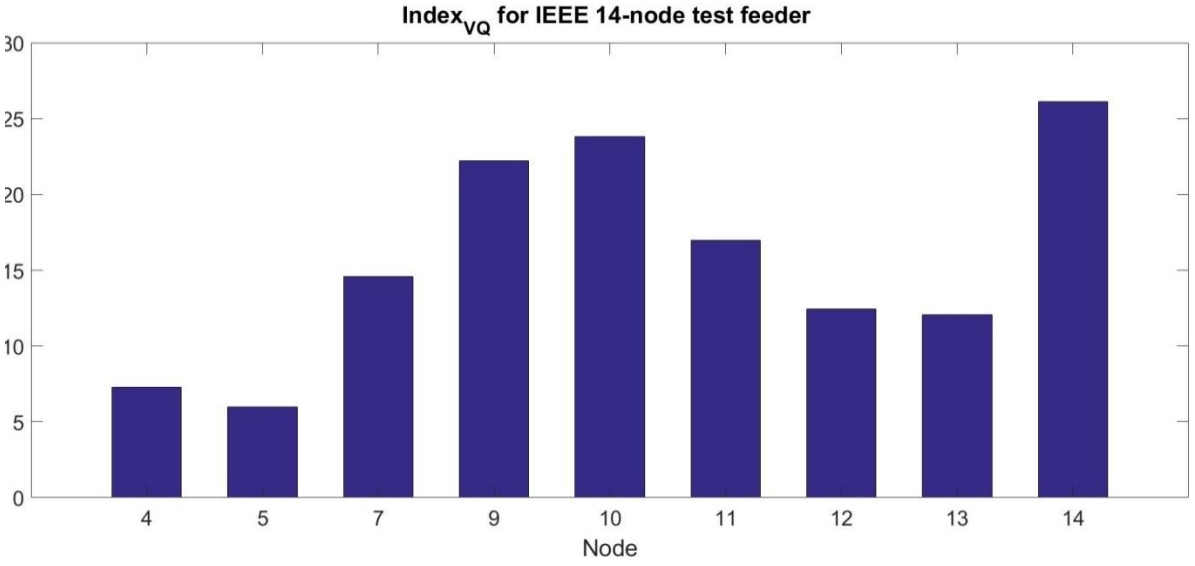

Figure 3. 6 Index_{VQ} of 14-node system

The results of $\text{Index}_{\text{P}}, \text{Index}_{\text{Q}}, \text{Index}_{\text{A}}$, and Index_{V} are shown in Figure 3. 7 - Figure 3. 10.

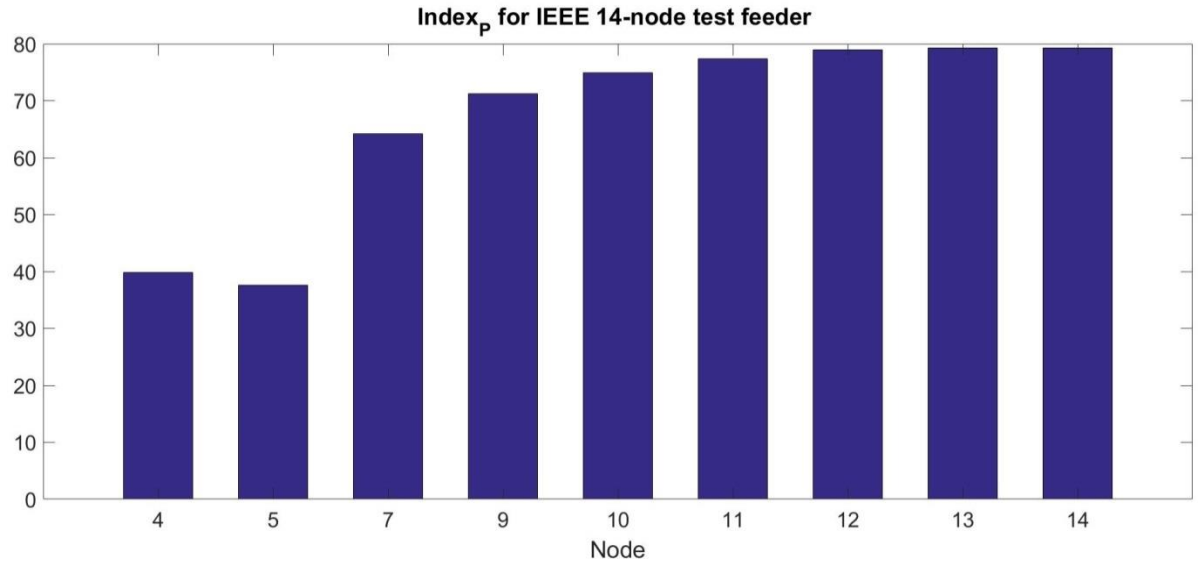

Figure 3. 7 Index$_P$ of 14-node system

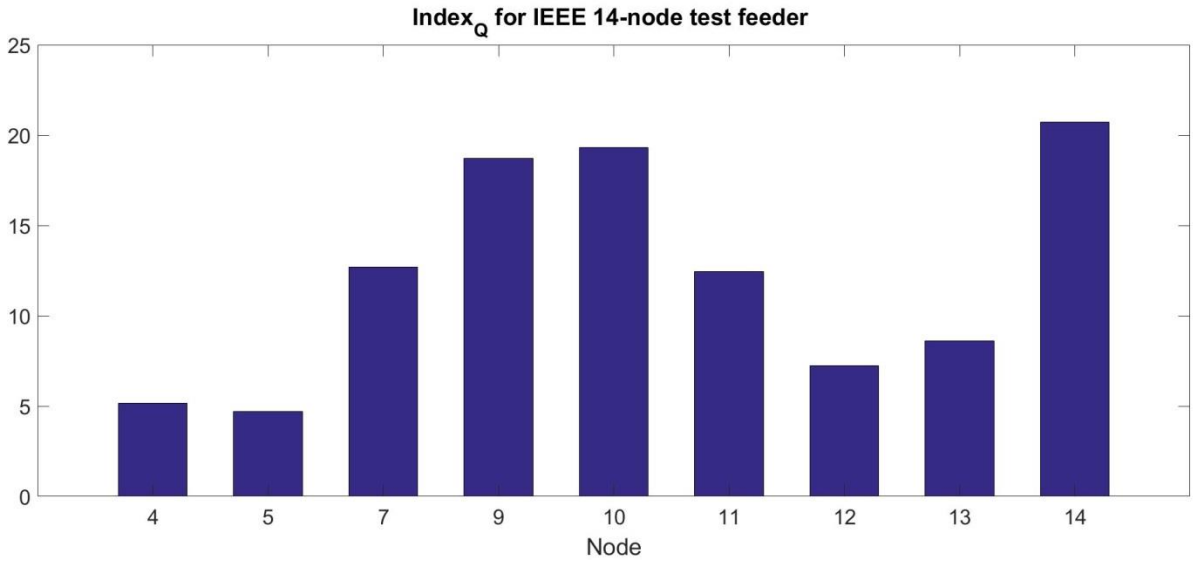

Figure 3. 8 Index$_Q$ of 14-node system

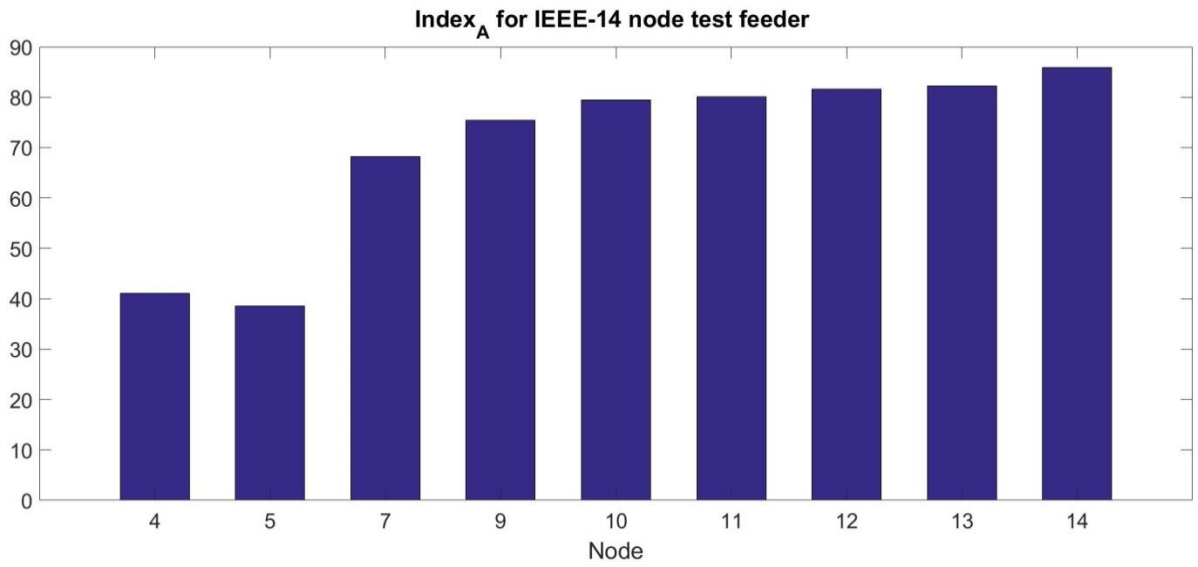

Figure 3. 9 Index_A of 14-node system

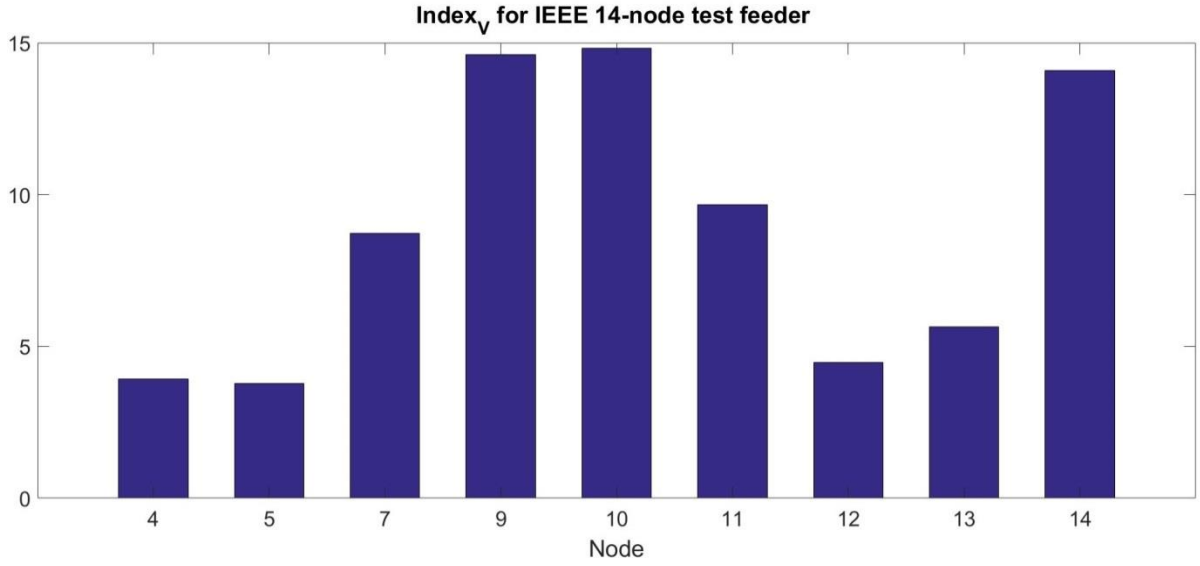

Figure 3. 10 Index_V of 14-node system

Result of Index_T is shown in Figure 3. 11. The Index_T represents the summation of Index_P and Index_Q.

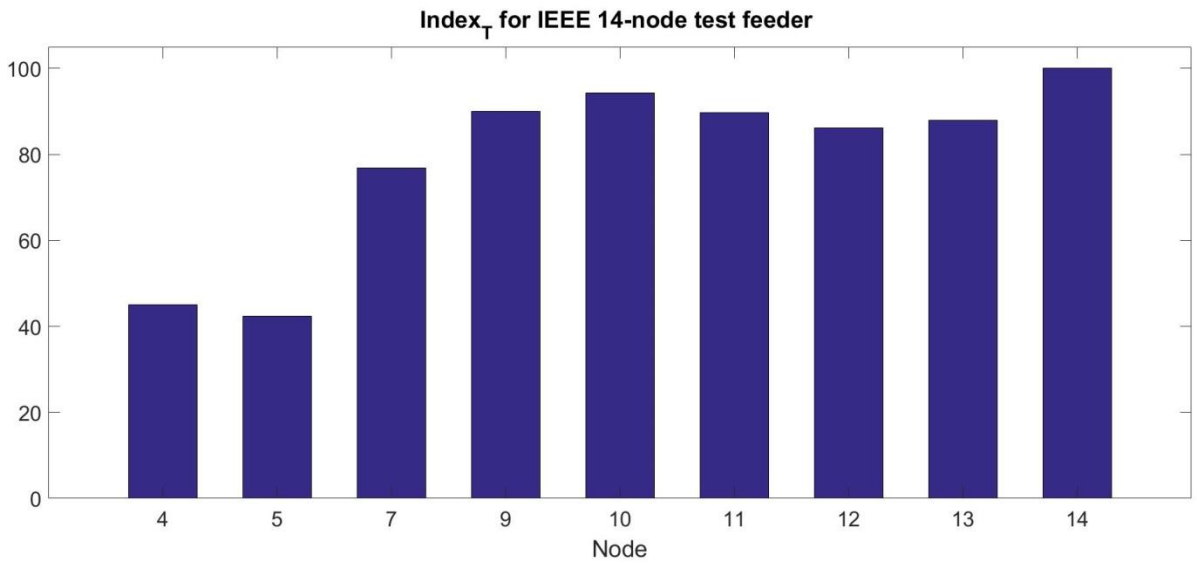

Figure 3. 11 Index$_T$ of 14-node system

Looking at Index$_P$ and Index$_A$, nodes 12, 13, and 14 have the highest values. Index$_P$ and Index$_A$ have a similar pattern. Index$_Q$ and Index$_V$ are similar as well, the highest nodes from these indices are 9, 10, and 14. The common top node between them is node 14 which is obtained from the result of Index$_T$. In other words, Index$_T$ suggested node 14 as the optimal node for storage placement. The storage system that is connected to the node would have the highest impact of regulating voltage angles and magnitudes.

CHAPTER 4 EVALUATION OF INDICES

From the previous discussions in chapter 3, the four basic indices can be obtained through the inverse of Jacobian matrix from Newton-Raphson method. Once the four basic indices have been calculated, five compound indices can also be obtained.

To verify the indices calculated for IEEE 14-node test feeder in chapter 3, an intensive case study has been conducted. A storage device is added to the system and it is moved from node to node. The default system without any storage is considered as the reference. For each installment of energy storage, the changed values of phase angle and voltage magnitude compared to the default case, have been recorded. Then the variation is compared with the indices to see if the variations of angle and magnitude have the same pattern of the indices.

The storage device is interfaced with grid through an inverter, both active and reactive power control can be done. That is to say that both active and reactive power can be injected from the point where the storage device is connected.

In this case, a storage device has moved along the nodes in the system. The output of storage device has changed from 100MW to 10MW and the injected of reactive power has changed in the range of 100MVar to 10MVar as well. To show how much the angle and magnitude have been affected by the active and reactive powers, the average variation in the

voltage angle and magnitude in every node has been summarized. The equations are shown in (4.1) and (4.2).

$$\text{Variation}_{|V|} = \frac{\sum_{i=1}^{N}\left(|V|_{iorg} - |V|_{inew}\right)}{\text{N}} \tag{4.1}$$

$$\text{Variation}_{\delta} = \frac{\sum_{i=1}^{N}\left(\delta_{iorg} - \delta_{inew}\right)}{\text{N}} \tag{4.2}$$

Where N is the number of nodes in system $|V|_{iorg}$ and δ_{iorg} are default angle and default magnitude at node *i* before adding any kind of energy storage system. $|V|_{inew}$ and δ_{inew} are angle and magnitude at node *i* after storage device connected. The summation of the variations in the angle and magnitude in every node can illustrate how much active and reactive power injection of a node can influence other nodes' angle and magnitude. The summation of variation in angle degree at every node is shown in Figure 4.1. Each line represents the cumulative impact of its corresponding node on other nodes for a wide range of injected active power. Although active power does not change the magnitude by much, the variation of voltage magnitude has shown in figure 4.2. The cumulative impact of voltage magnitude with active power injected in different nodes shown as lines.

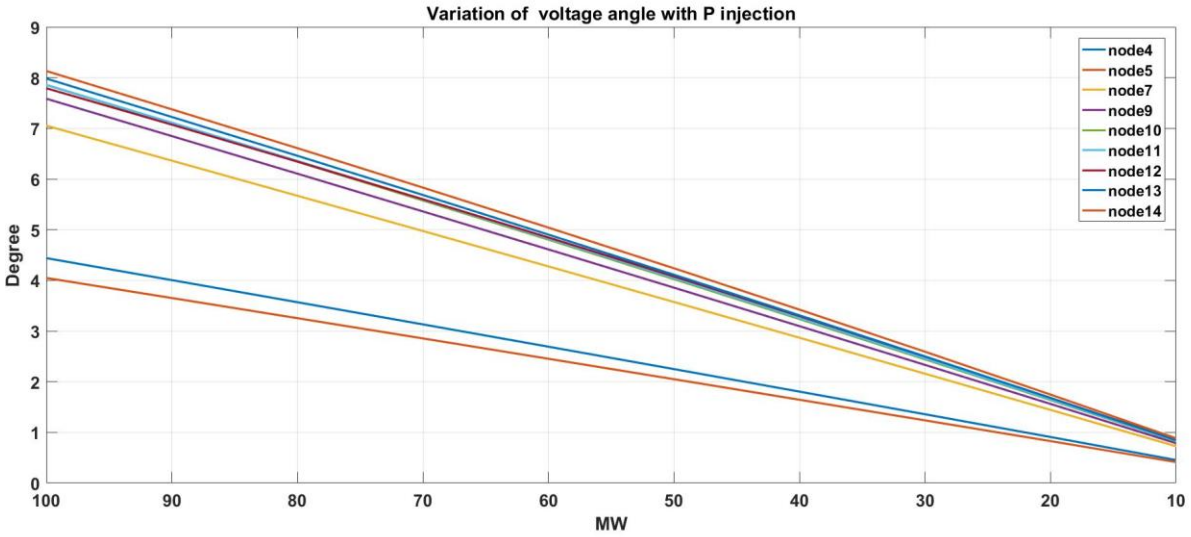

Figure 4. 1 The cumulative variation of angles for a range of active power

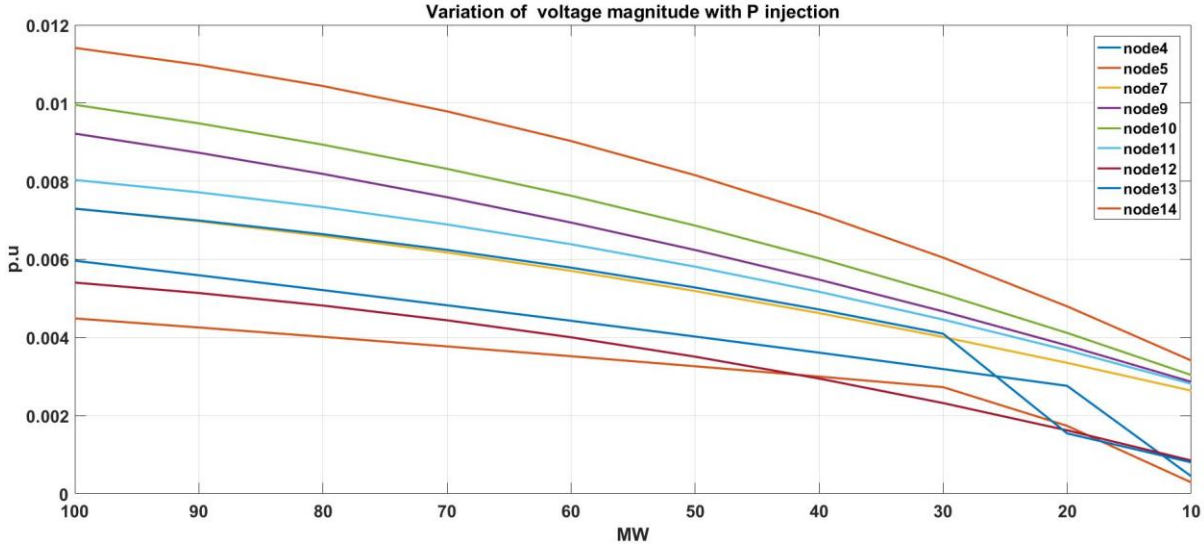

Figure 4. 2 The cumulative variation of magnitudes for a range of active power

The variation in voltage angle and magnitude while Q injection has shown in figure 4.3 and figure 4.4.

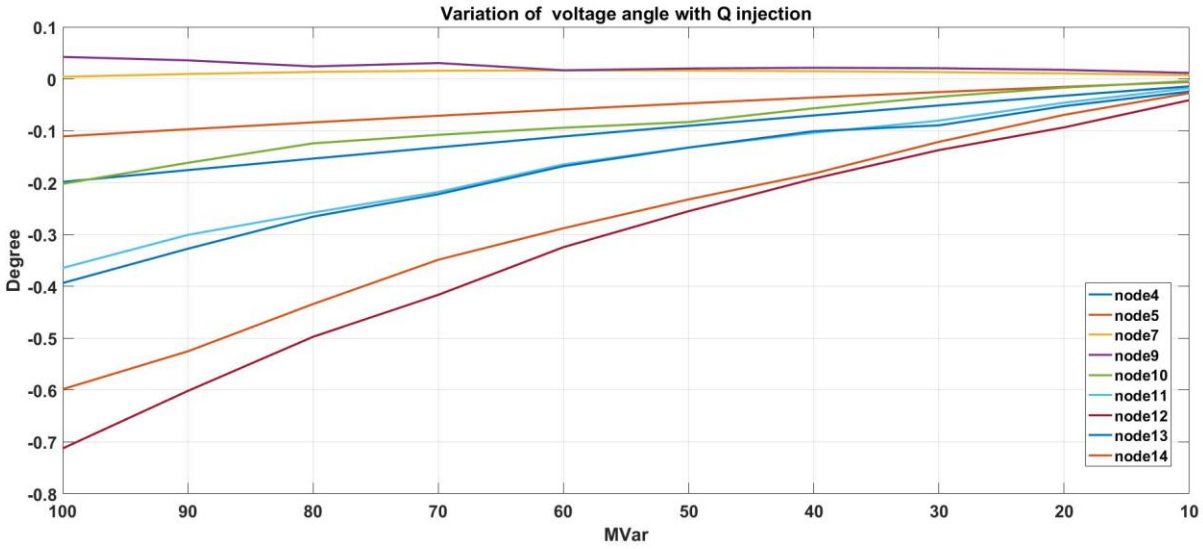

Figure 4. 3 The variation of angle while Q injection

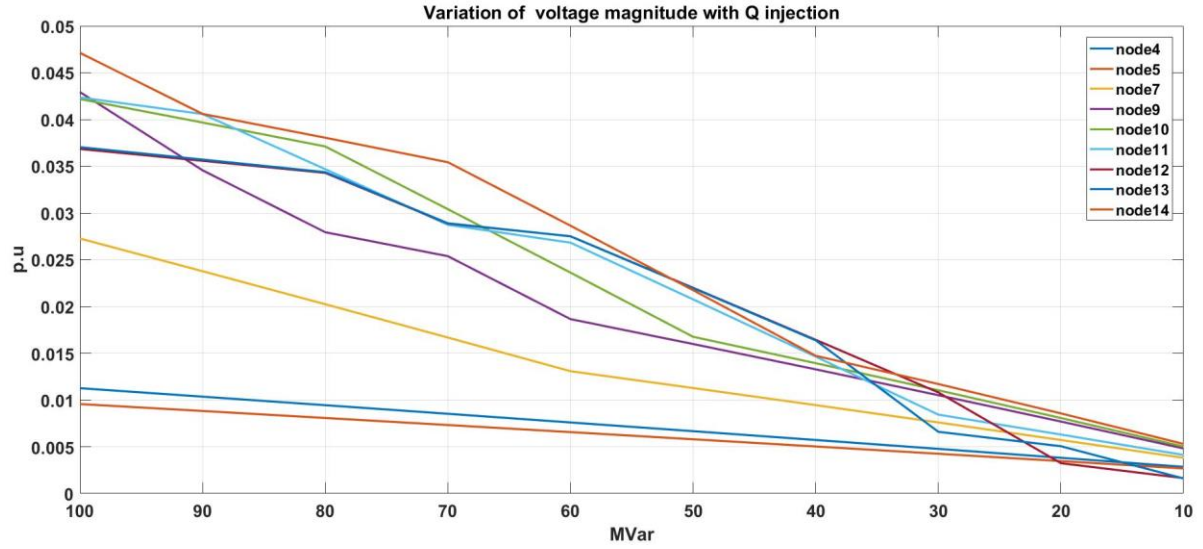

Figure 4. 4 The variation of magnitude while Q injection

The variation of voltage angle and magnitude while apparent power injection has shown in Figure 4. 5 and Figure 4. 6.

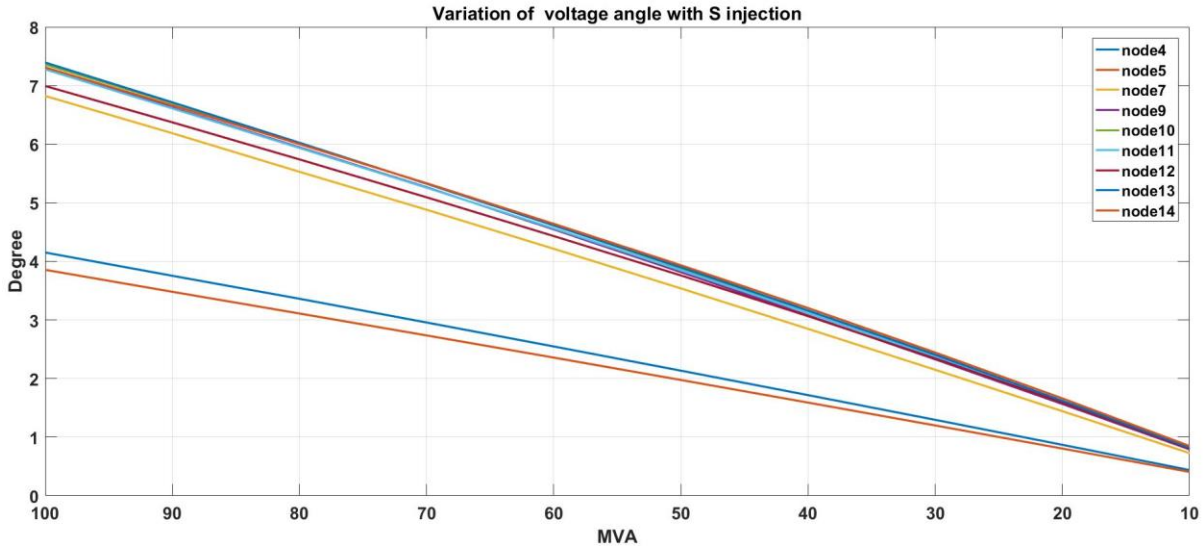

Figure 4. 5 The variation of angle while S injection

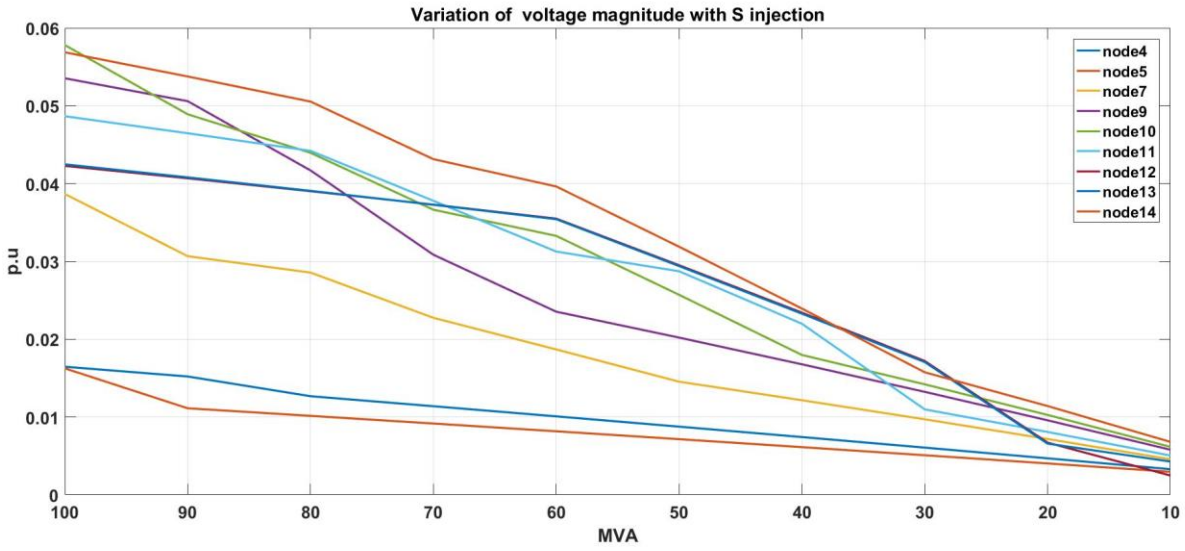

Figure 4. 6 The variation of magnitude while S injection

From Figure 4.1 and Figure 4.3, the angle is more affected by the change on active power than reactive power. Figure 4.2 and Figure 4.4 show that the voltage magnitude is more sensitive to reactive power than active power.

To evaluate that the indices calculated in chapter 3 are reliable and able to reflect the sensitivity of angle and magnitude, a comparison is made. The summation of variation in angle and magnitude in every node when 20 MVA is injected at various nodes, is compared with the indices that proposed in chapter 3.

Index_A is defined as Index_{AP} subtract Index_{AQ}, which represent the influences of the active power on the angle. Index_P is the angle's sensitivity to the active power. The Index_A and Index_P compared with the variation on voltage angle is shown in Figure 4.7. The active power injection is considered as 20MW. The values of variation of actual angle and indices are scaled with the reference of node 14 to see if they are in the same pattern.

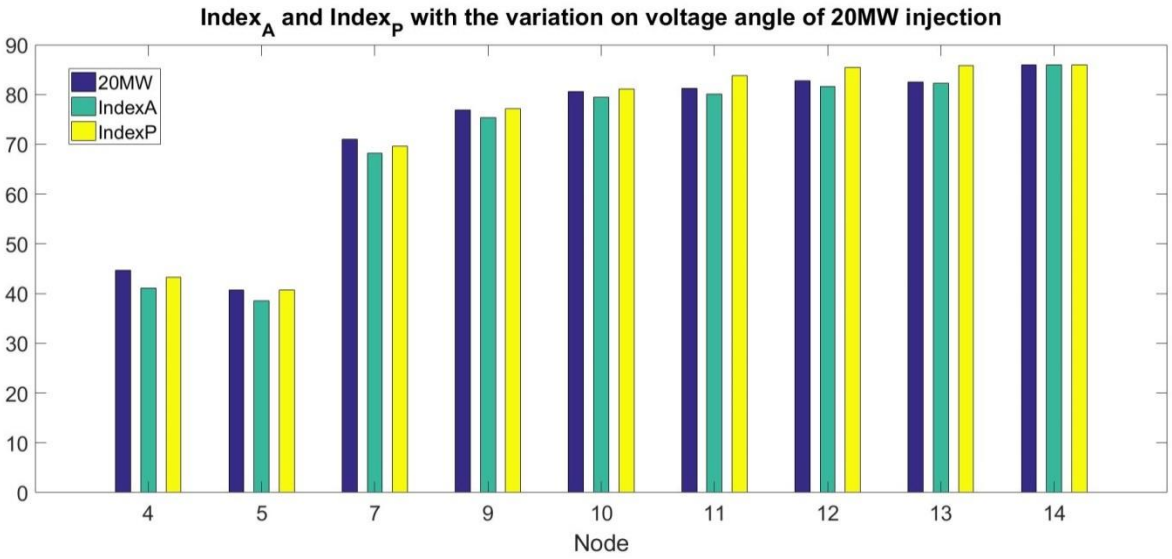

Figure 4. 7 Index_A and Index_P compared with the variation of voltage angle

Index_V is defined as Index_{VQ} subtract Index_{VP}, that represent the influences of reactive power injection on voltage magnitude. The comparison of Index_Q, Index_V and the variation in voltage magnitude is shown in Figure 4.8.

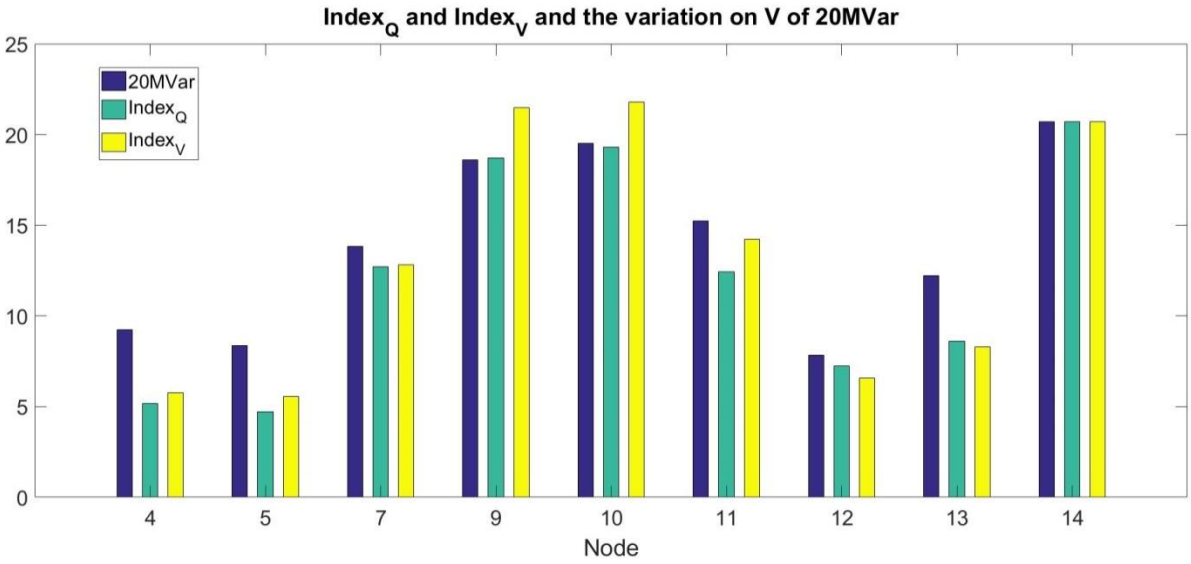

Figure 4. 8 The comparison of Index_V, Index_P and the variation on voltage magnitude

In Figure 4.9, the variation of both of the angle and magnitude of 20 MVA with apparent power injected is compared with Index_T. Again, the node 14 is selected as the base, values of variation and index are in the same scale. Since Index_T is the summation of two dominant indices and subtraction of non-dominant indices, the variation of angle and magnitude are summarized and compared with Index_T.

Figure 4. 9 Index$_T$ compared with the total variation of angle and magnitude

With the increasing of injection, the variations of the angle and magnitude become less related to the Index, the variations of the angle and magnitude in some of the nodes increase rapidly rather than following the Index. The variations increase, especially happen to the voltage magnitude. In Figure 4. 6, the voltage magnitude in node 9 raised rapidly while the injection excess 60 MVA. In Figure 4.7 – 4.9, the variations still following the similar pattern with the proposed indices though 20 MVA is a significant power injection for the IEEE 14-node test feeder.

CHAPTER 5 INDICES OF IEEE 123-NODE TEST FEEDER

5. 1 IEEE 123-node test feeder

IEEE PES Distribution System Analysis Subcommittee's Distribution Test Feeder Working Group has released several test feeders. The IEEE 123-node test feeder is selected as an expansion testing system for sensitivity analysis. The system is shown in Figure 5. 1.

The IEEE 123-node test feeder operates at a nominal voltage of 4.16 kV. The test feeder has different types of conductors including overhead and underground lines, the main feeder is overhead three-phase.

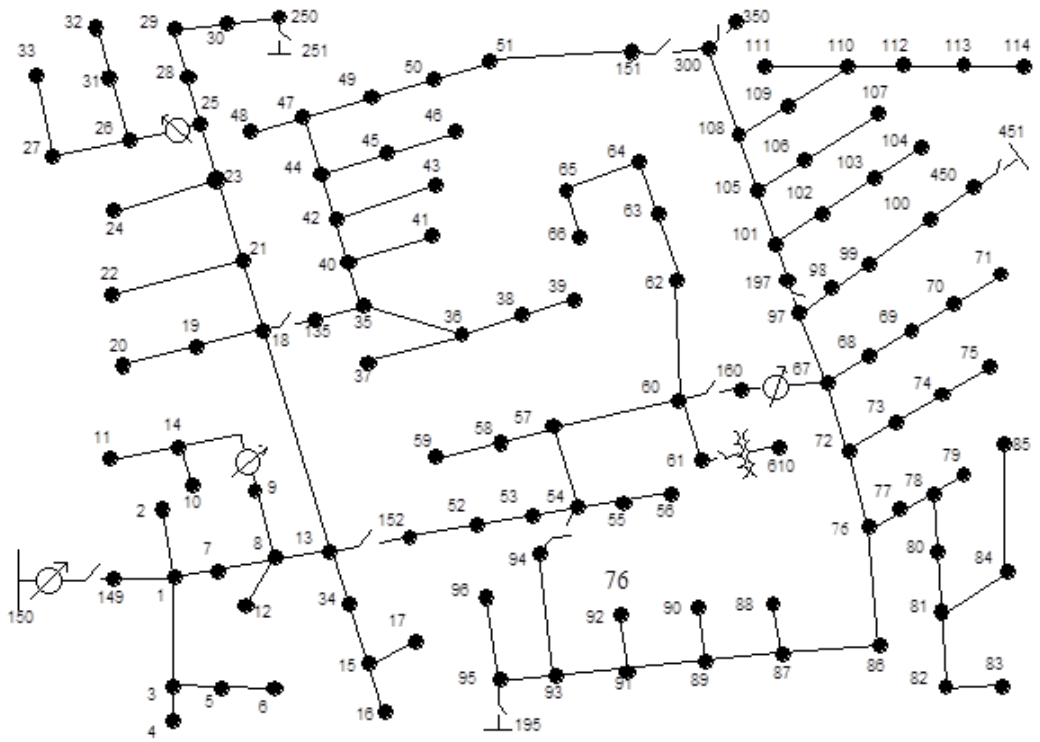

Figure 5. 1 IEEE 123-node test feeder

Some of the nodes are renumbered to keep the total node numbers within 123. This modification is done for the sake of computer programing and the original numbers are still visible in Figure 5. 2 with a gray color.

The slack bus is node 115. Switches in the system are all closed, but the switches connected to node 195, 250, 350, and 451 which connect IEEE 123 network to other possible networks are open. All changes have done to nodes are listed in Table 5. 1, there are 122 nodes remain after the renaming.

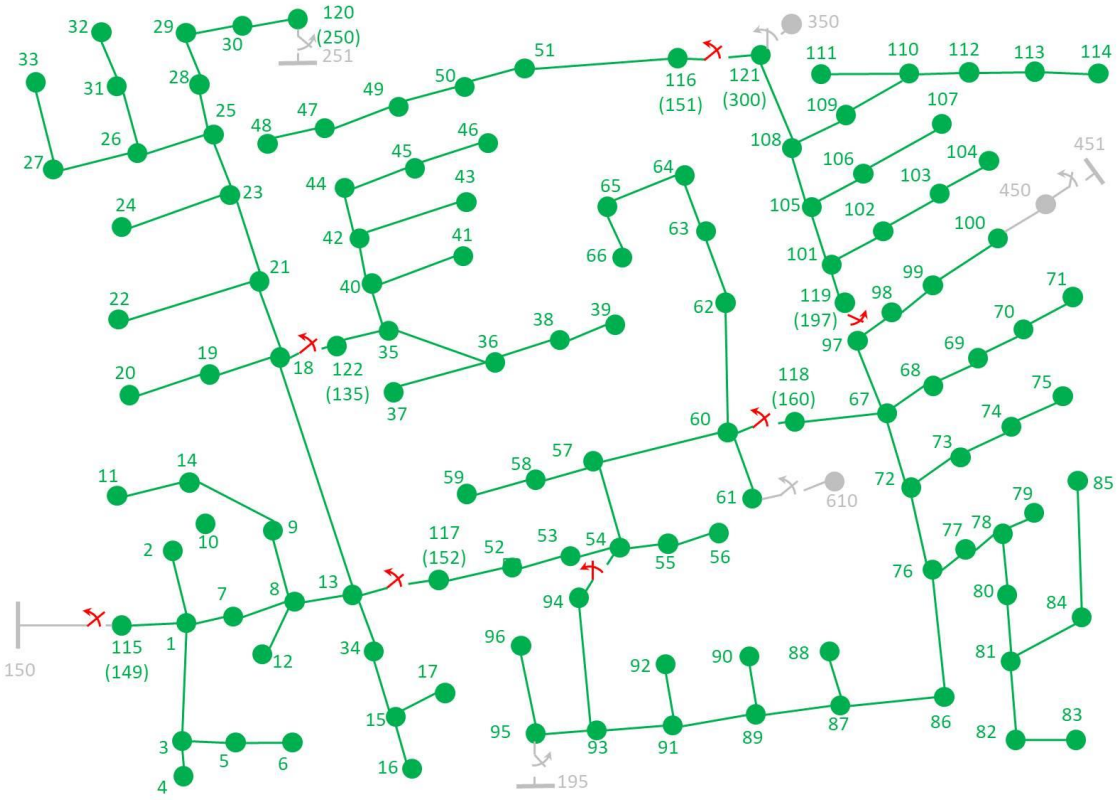

Figure 5. 2 IEEE 123-node test feeder after modify

Table 5. 1 Node changed from IEEE 123-node test feeder

Node	Change	Node	Change
150	Removed	195	Removed
149	115	160	118
135	122	610	Removed
250	120	300	121
251	Removed	151	116
152	117	450	Removed
451	Removed	197	119

Some of loads in the network are single phase. For the sake of this study, they are replaced with equivalent three-phase loads.

5. 2 Sensitivity indices of IEEE 123-node test feeder

In the case of IEEE 123-node test feeder, Newton-Raphson iteration is processed and obtained the Jacobian matrix of IEEE 123-nod. The four basic indices are calculated from the inverse of Jacobian matrix. Since there is no PV bus exist in IEEE 123-node test feeder, every node is considered as the potential candidate, there is no need to reduce the size of sub-matrices. Every index is presented in percentage. The greater value means the node is a suitable location for a storage device according to indices. The four basic proposed indices are shown in Figure 5.3 – 5.7.

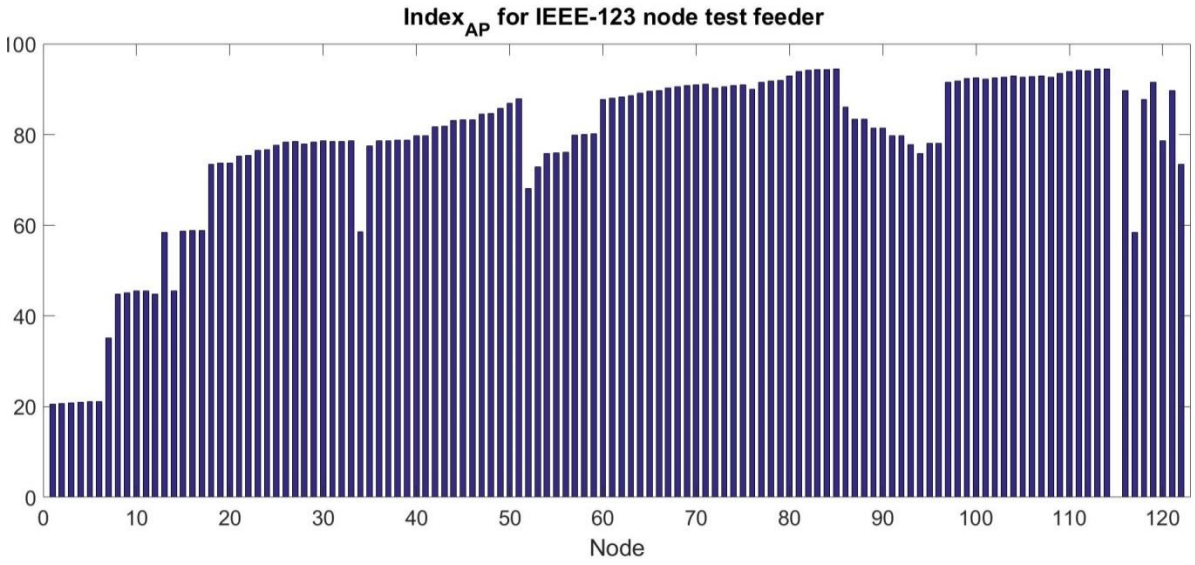

Figure 5. 3 Index$_{AP}$ of IEEE 123-node test feeder

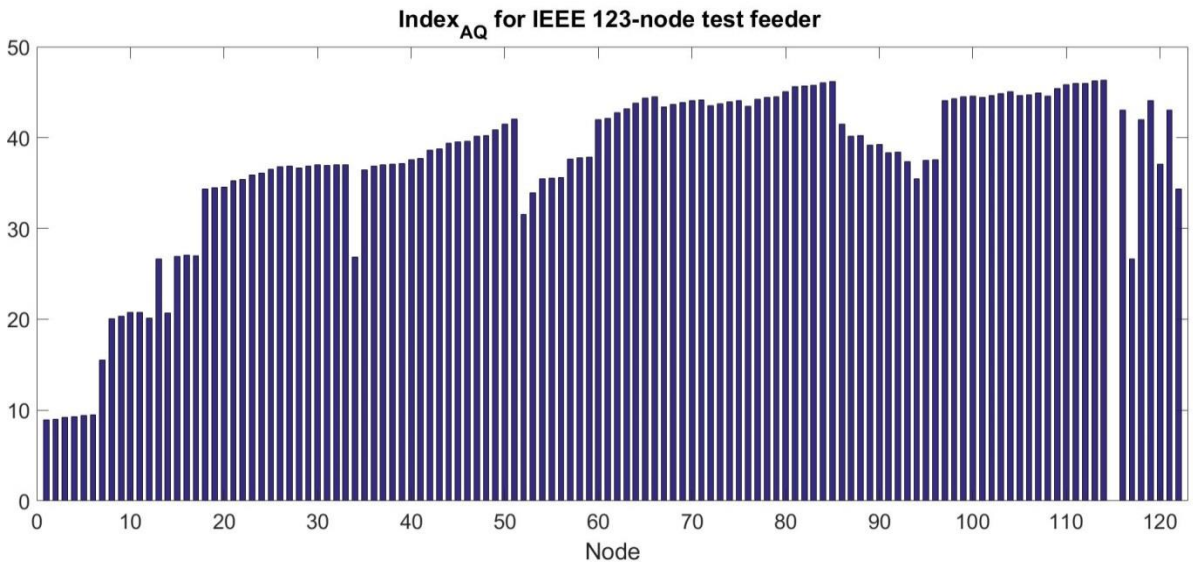

Figure 5. 4 Index$_{AQ}$ of IEEE 123-node test feeder

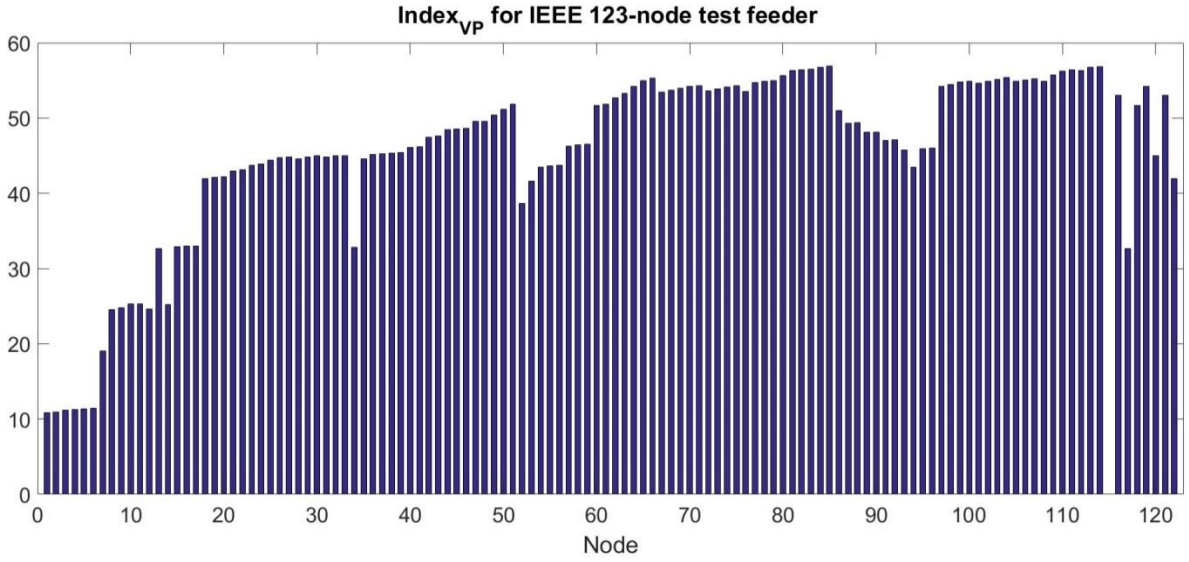

Figure 5. 5 Index$_{VP}$ of IEEE 123-node test feeder

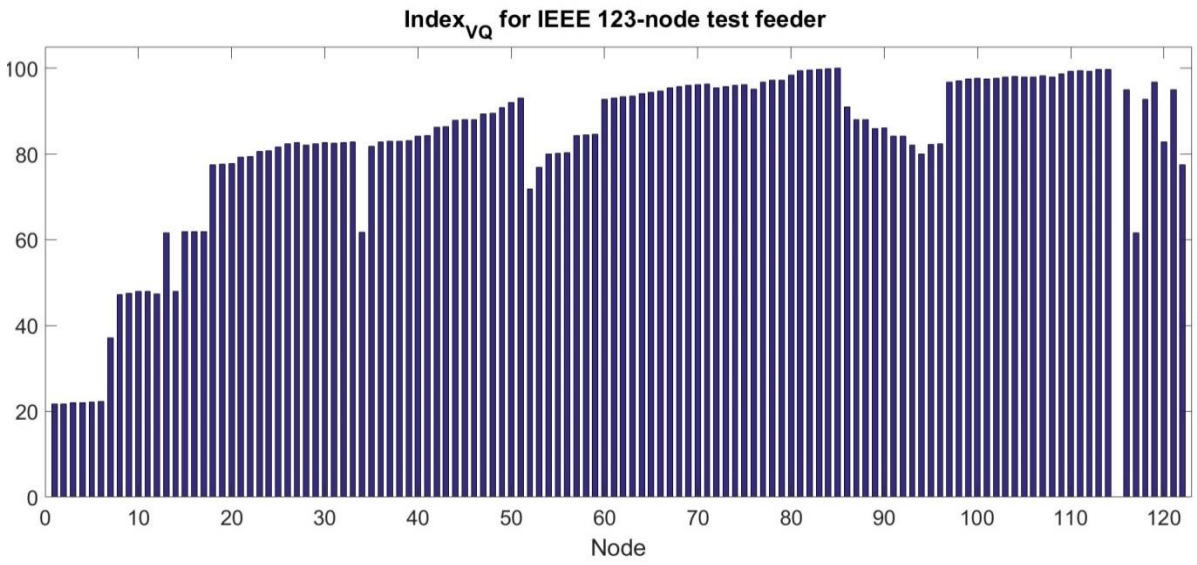

Figure 5. 6 Index$_{VQ}$ of IEEE 123-node test feeder

The results of Index$_{\mathrm{P}}$, Index$_{\mathrm{Q}}$, Index$_{\mathrm{A}}$, and Index$_{\mathrm{V}}$ are shown in Figure 5. 7- Figure 5. 10.

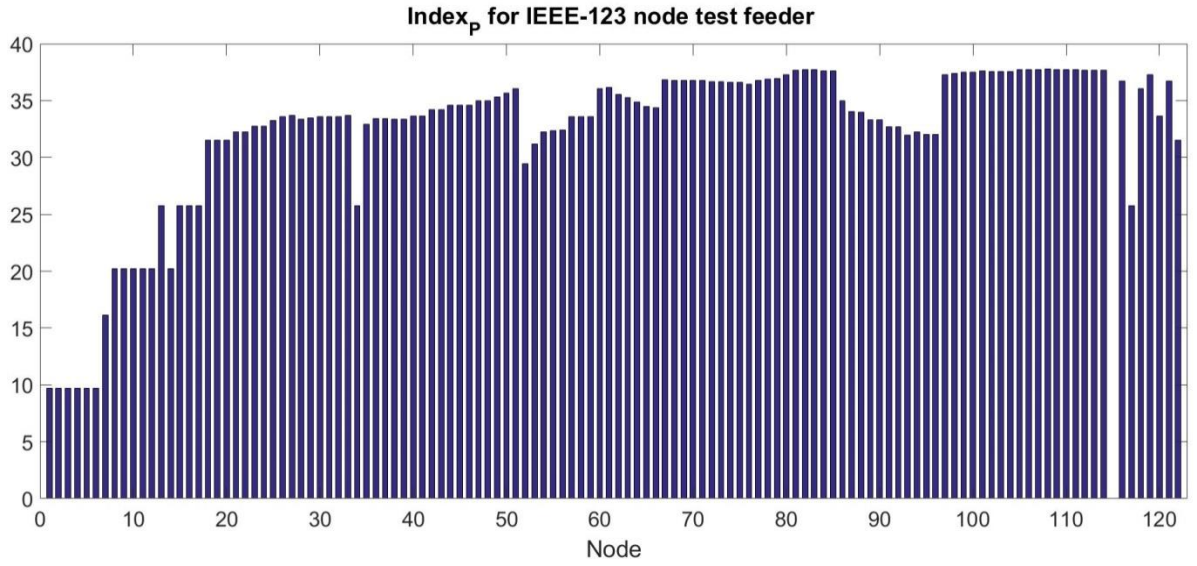

Figure 5. 7 Index$_{P}$ of IEEE 123-node test feeder

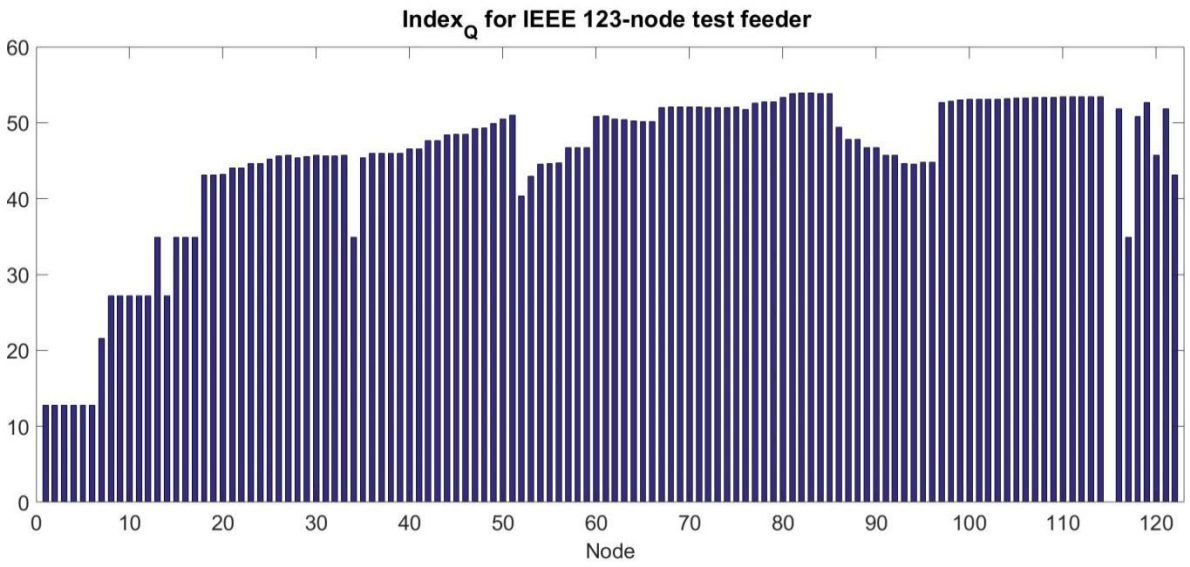

Figure 5. 8 Index$_Q$ of IEEE 123-node test feeder

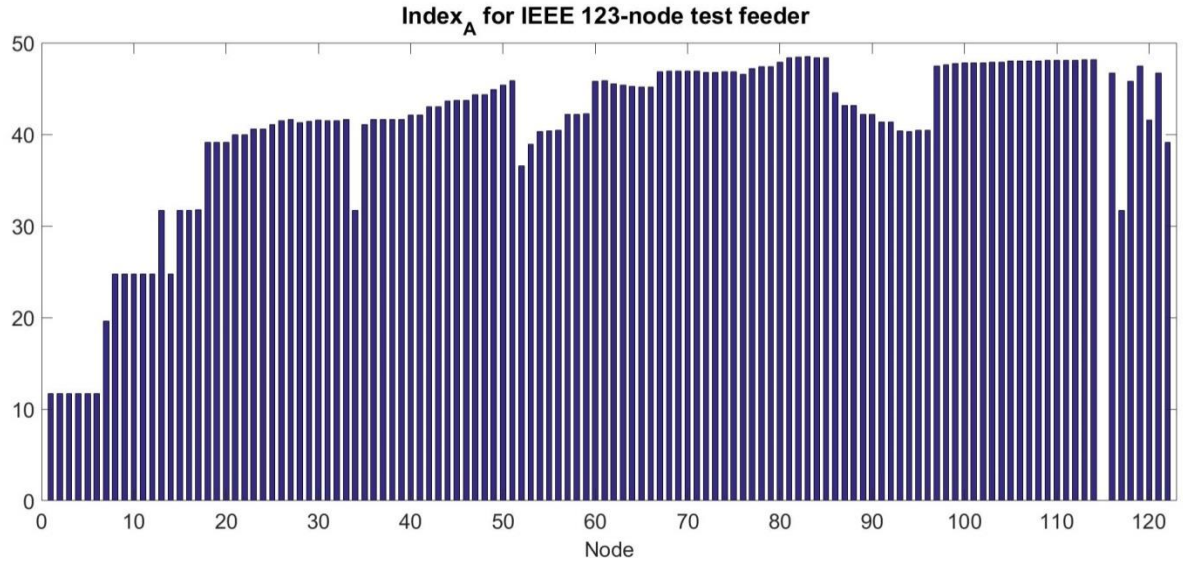

Figure 5. 9 Index$_A$ of IEEE 123-node test feeder

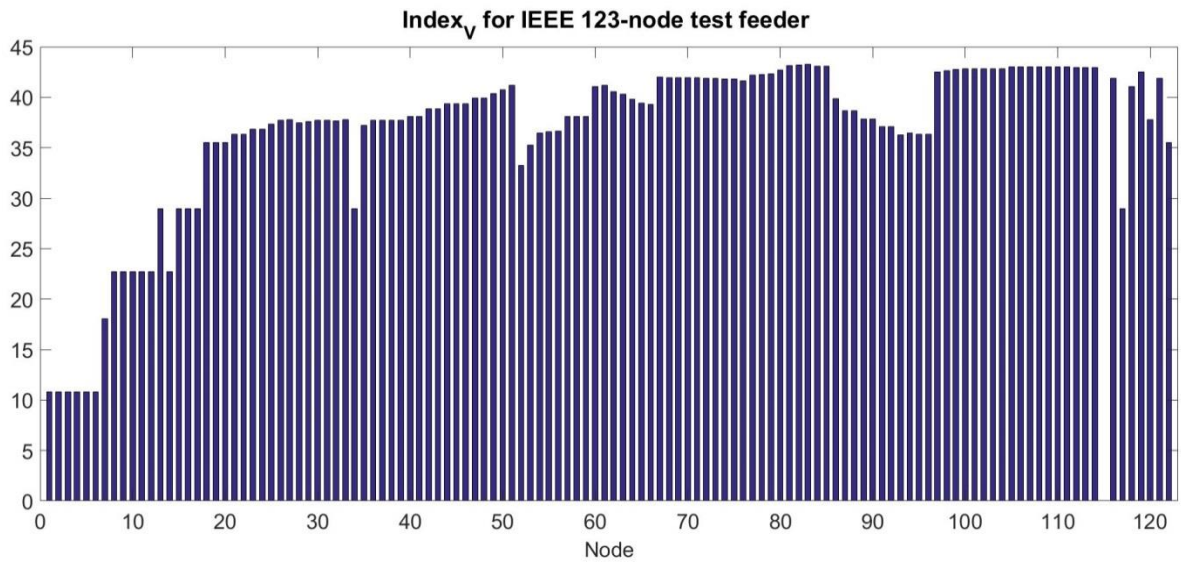

Figure 5. 10 Index$_V$ of IEEE 123-node test feeder

The total index, Index$_T$ is shown in Figure 5. 11. In Index$_T$, the node with the highest sensitivity index value is node 83.

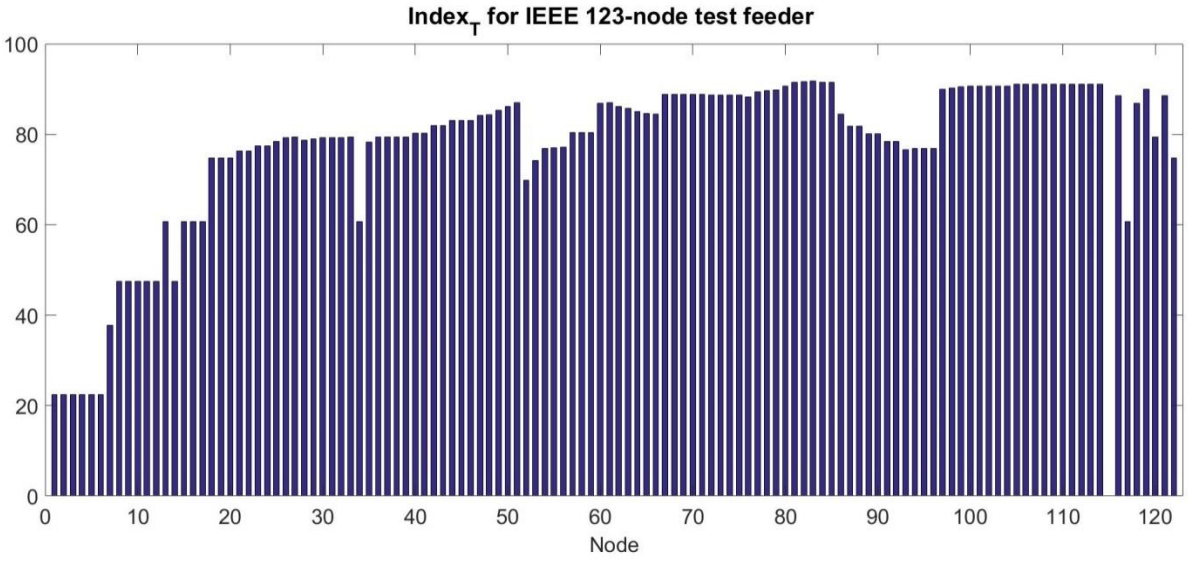

Figure 5. 11 Index$_T$ for IEEE 123-node test feeder

As the evaluation in chapter 4, the 20MW active power injected and moved all over the nodes. The variation of voltage angle in all nodes are summarized and compared with Index_P and Index_A. The variation of voltage angle, Index_P, and Index_A are all set as the same scale as the last node in the system. The result is shown in Figure 5. 12.

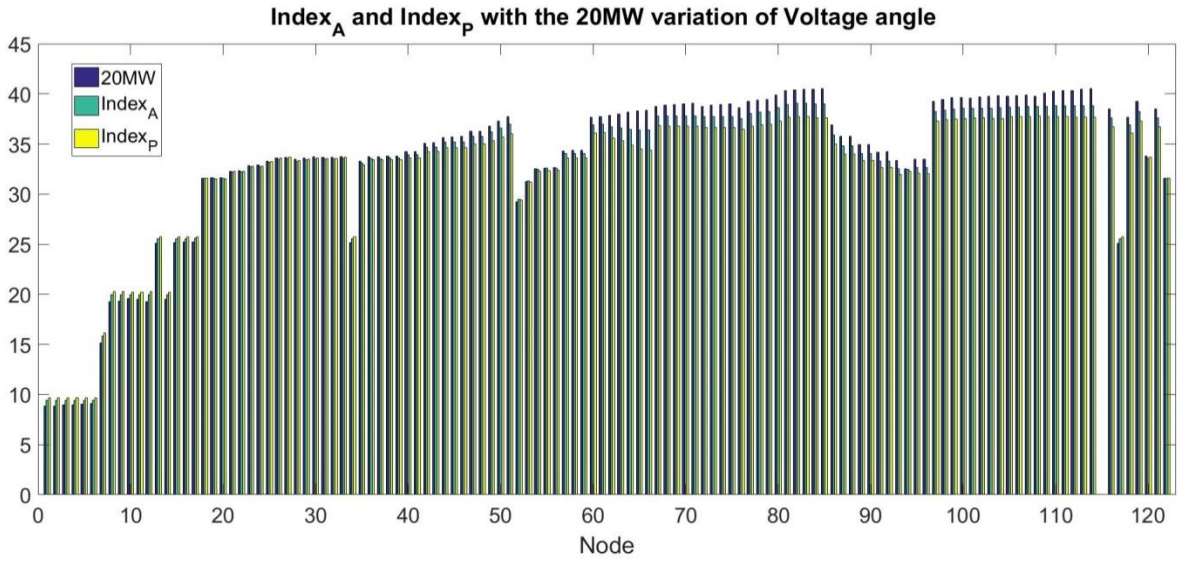

Figure 5. 12 The variation of voltage angle, Index_P and Index_A

The 20 MVar reactive power injected is compared with Index_Q and Index_V on voltage magnitude variation is shown in Figure 5.17.

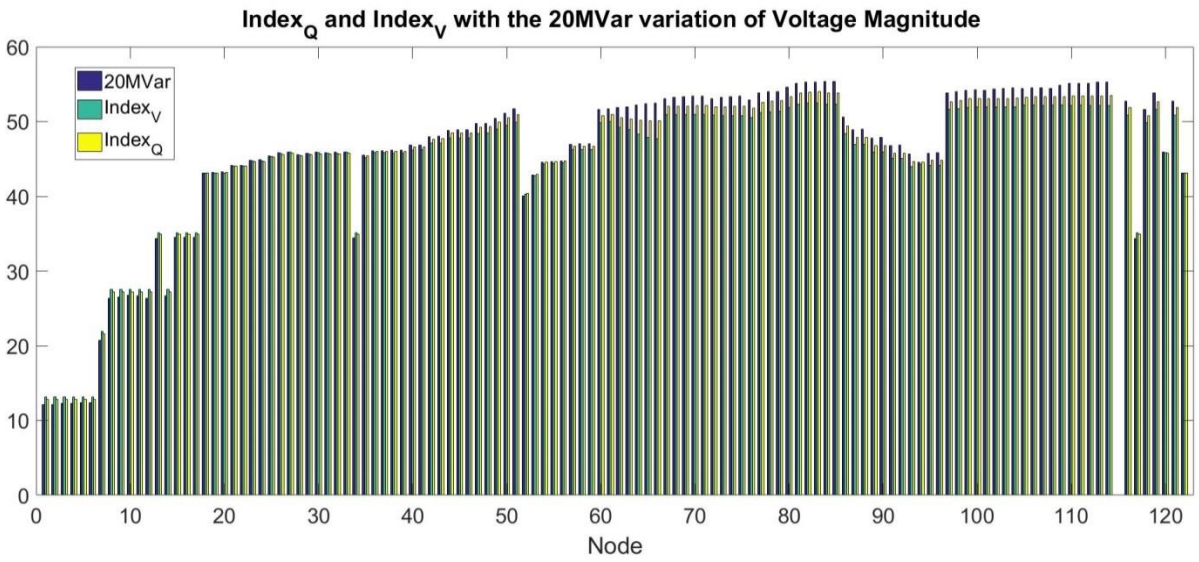

Figure 5. 13 Index_Q and Index_V with the 20 MVar variation of Voltage Magnitude

The Index_T is compared with the summation of voltage angle and voltage magnitude variation and shown in Figure 5. 14 .

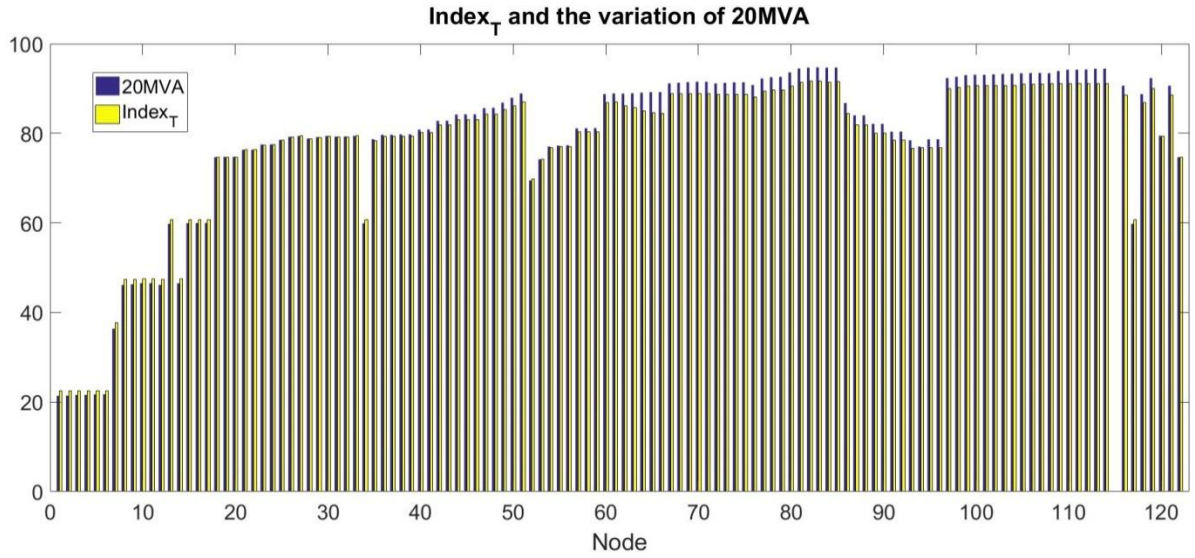

Figure 5. 14 Index_T and the variation of 20MVA

The testing is done and the values of variation of voltage magnitude and angle are obtained. The results show that the variation of voltage magnitude and angle both have the highest value in node 83 just as Index_T has suggested. The second highest is node 114, the location of node 83 and node 114 are shown in Figure 5. 15.

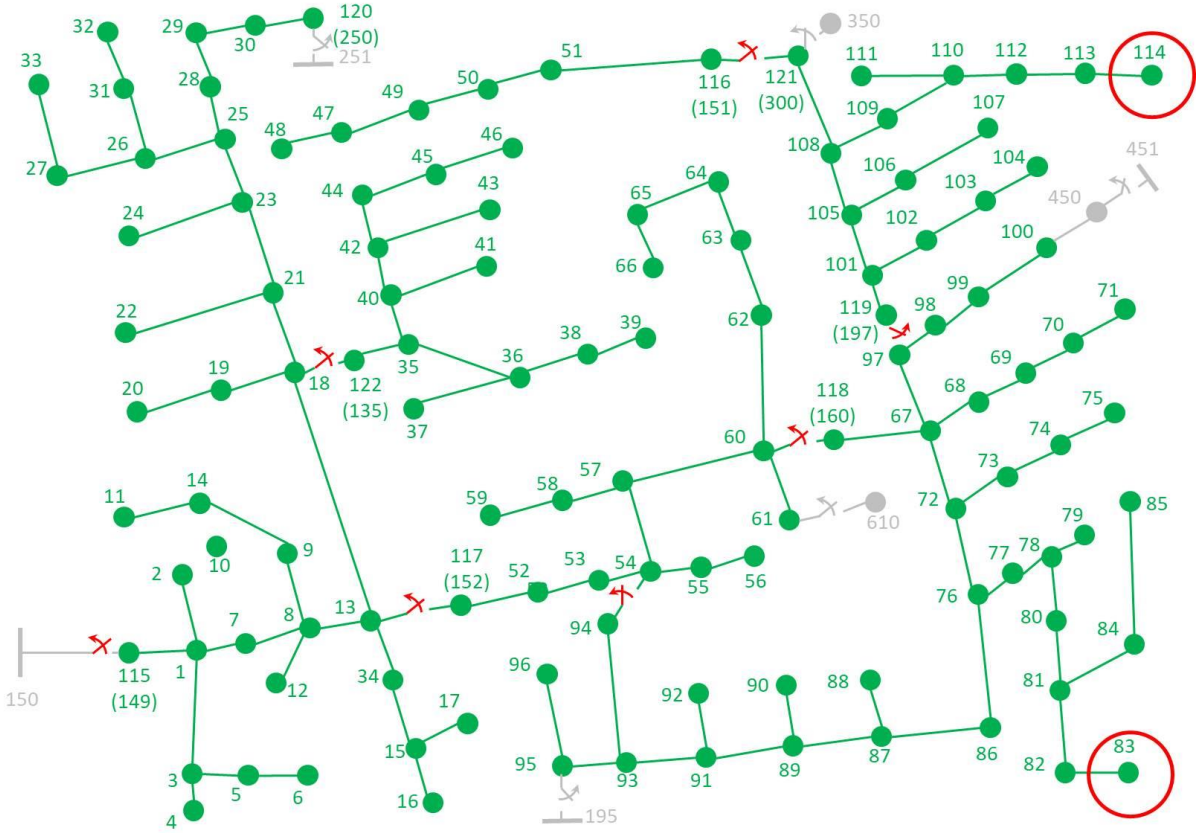

Figure 5. 15 Nodes with high variation in IEEE 123-node

Both node 83 and node 114 could be a suitable location for storage placement; both nodes have high index value. A storage device that connected to these nodes could regulate voltage angle and magnitude with the highest impact. If the node with the highest index value

is not able to install a storage device, the nearby nodes with similar index value can also be considered as suitable locations and will have close performance.

In order to show that nodes suggested by the index are suitable locations for storage placement, node 83, 114, 67, and 13 have been selected. Since node 83 and 114 are relatively far from the utility feeder, a node that is closer to slack bus and a node at the middle distance from the slack bus are selected and compared with each other for different power input. The result of variation in voltage angle with active power injection is shown in Figure 5. 16. Node 83 and 114 have very close index value so they may look likes one line in the following figure.

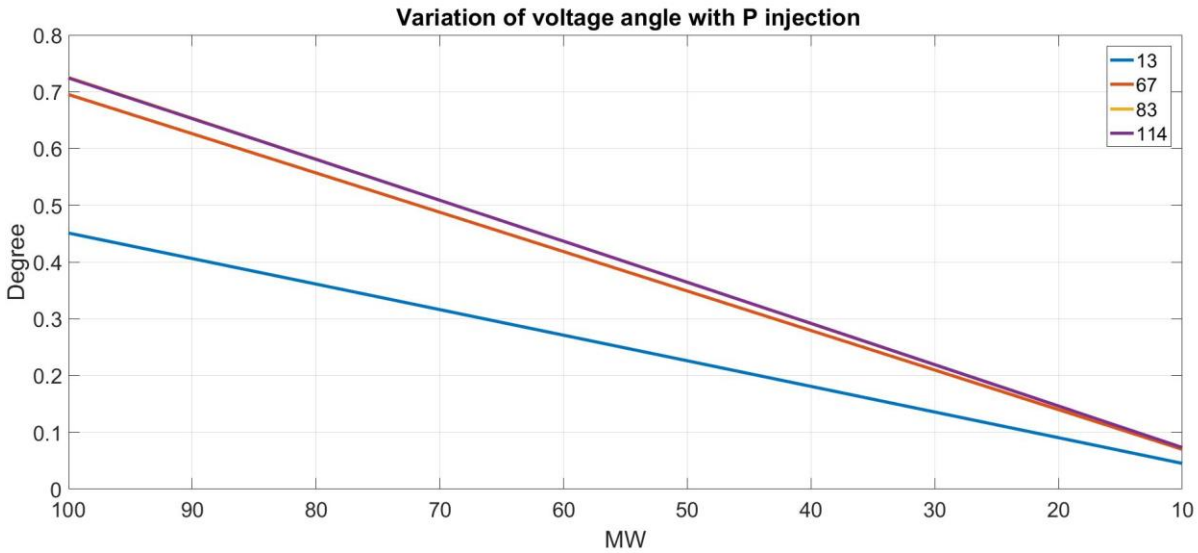

Figure 5. 16 Variations of voltage angle with active power injection on IEEE 123-node test feeder

Variation of voltage magnitude with active power injection on IEEE 123-node test feeder is shown in Figure 5. 17.

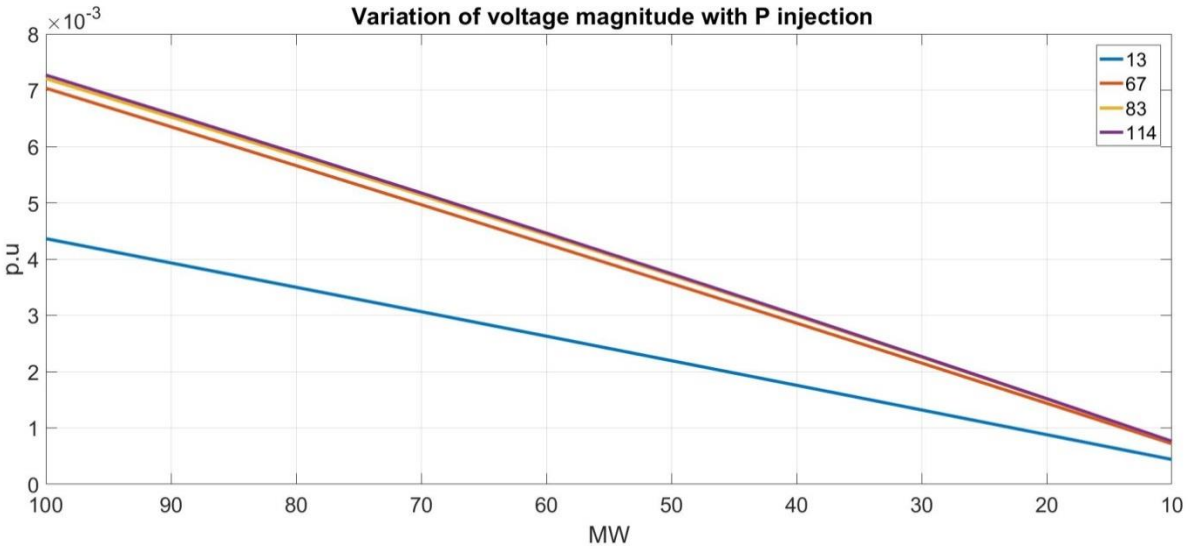

Figure 5. 17 Variation of voltage magnitude with active power injection on IEEE 123-nodes test feeder

Variation of voltage angle and magnitude with reactive power injection are shown in Figure 5. 18 and Figure 5. 19.

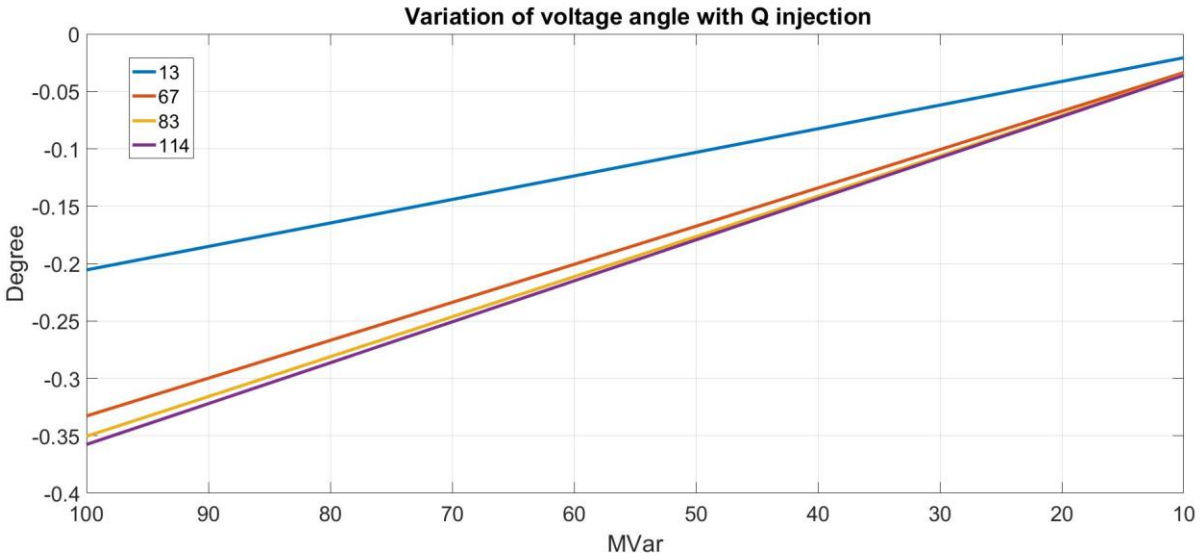

Figure 5. 18 Variation of voltage angle with reactive power injection on IEEE 123-node test feeder

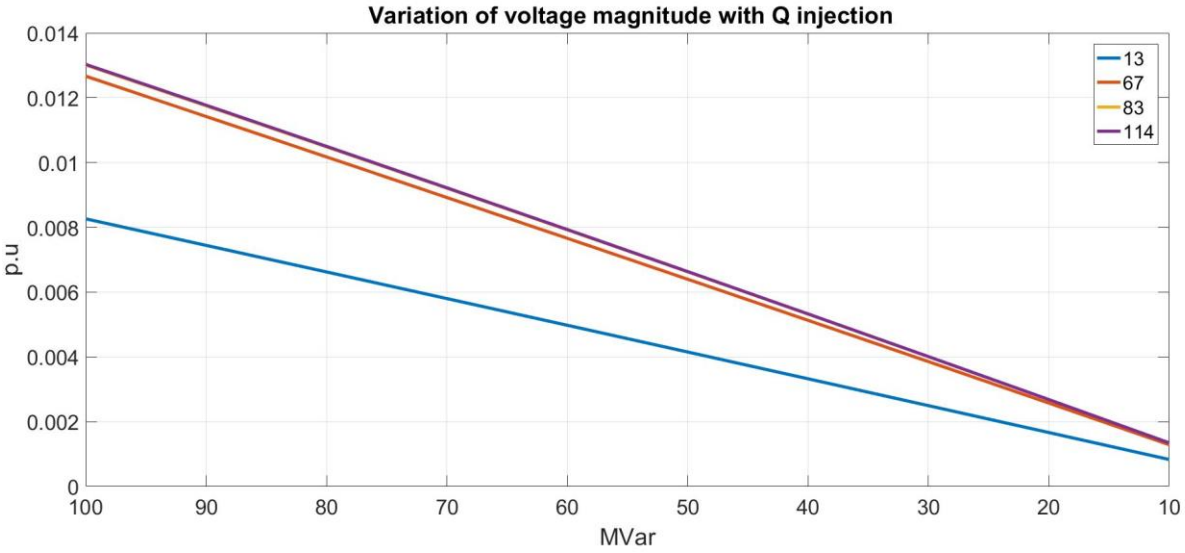

Figure 5. 19 Variation of voltage magnitude with reactive power injection on IEEE 123-node test feeder

Variation of voltage angle and magnitude with apparent power injection are shown in Figure 5. 20 and Figure 5. 21.

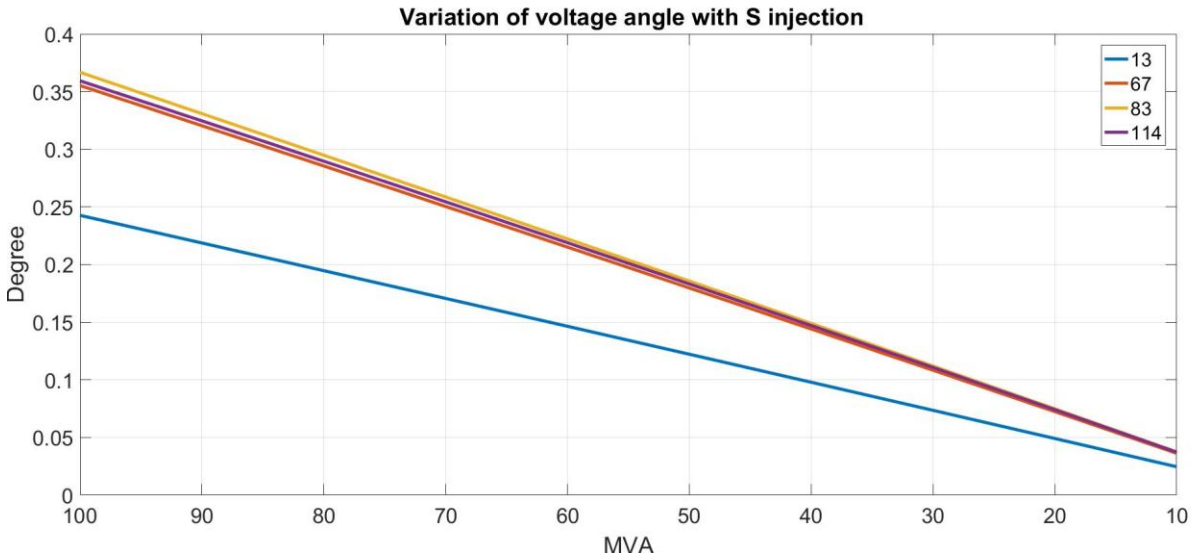

Figure 5. 20 Variation of voltage angle with apparent power injection on IEEE 123-node test feeder

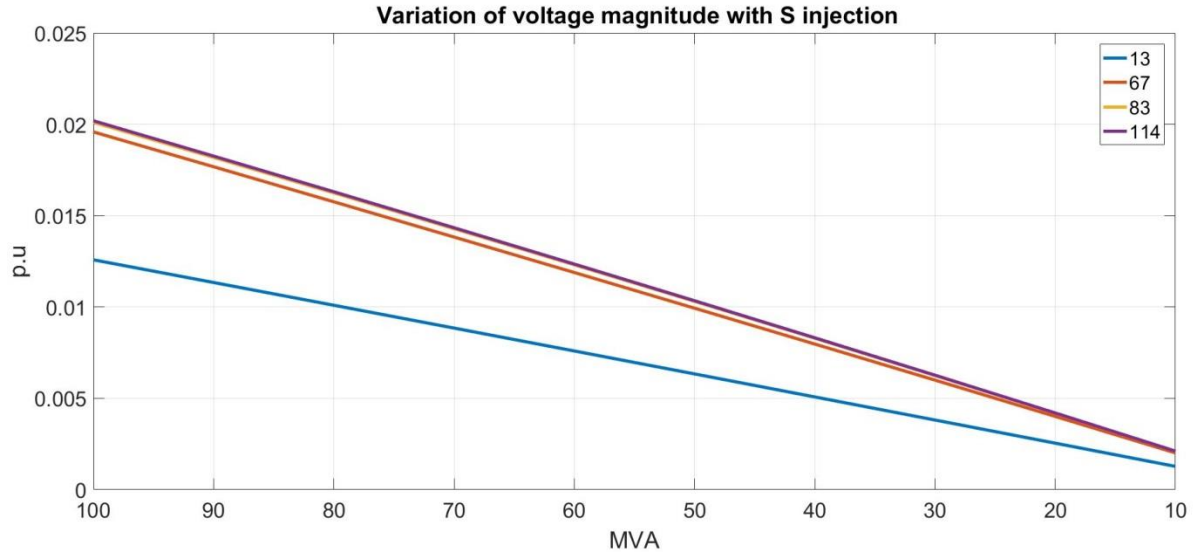

Figure 5. 21 Variation of voltage magnitude with apparent power injection on IEEE 123-node test feeder

In Figure 5. 16, Figure 5. 18, and Figure 5. 20 which are corresponding to the $Index_A$ and $Index_P$, active power makes more impact to the cumulated variation of the angle than reactive power. Node 114 and 83 can make the greatest impact on the voltage angle and the

following nodes are node 67 and 13. In both of the figure, node 114 and 83 have similar results on the impact of voltage angle. The impact that node 13 can make is lower than node 114, 83, and 67. The impact of node 114 on the angle compared to node 83 is slightly higher in Figure 5. 18, lower in Figure 5.20 and about the same in Figure 5. 16.

In Figure 5. 17, Figure 5. 19, and Figure 5. 21, reactive power makes more impact to voltage magnitude compared to the active power. The results are also corresponding to the $Index_Q$ and $Index_V$. Node 114 and 83 have almost the same and the highest impact on voltage magnitude compared to node 67 and 13. The impact of node 13 also far behind from node 114, 83, and 67. The suggested nodes by the sensitivity indices have a higher impact than any other random nodes.

CHAPTER 6 CONCLUSIONS AND FUTURE WORKS

6. 1 Conclusion

Storage systems are critical to the distribution system, since they provide active and reactive power to improve both of the angle and voltage magnitude, absorb excessive power and provide power support in time of need. However, storage devices are expensive and cannot be installed on every node in the system. Finding the optimal location for a storage system that can impact the whole system is necessary. In this study, sensitivity indices are proposed for analyzing the optimal location for the storage system. The indices are obtained from the inverse of Jacobian matrix which can be calculated through the Newton-Raphson power flow methodology. Once the Newton-Raphson iteration is converged, no other iteration is required for the suggested method for finding the optimal locations. This is different from other approach in references [29], [32], [36], and [37]. Having the inverse of Jacobian matrix, PV nodes are removed from the matrix and reach four equal-sizing sub-matrices. The four basic indices can be calculated from these four sub-matrices.

The sensitivity indices can be generated in a simple and fast manner. These indices quantify the impact of active and reactive power on any node of the system on the overall angle and magnitude of the network. Therefore the optimal storage location is corresponding to the node with the highest index. The sensitivity of voltage angle and magnitude to activive

power and reactive power is a key for this method. The four basic indices are listed in Table 6. 1.

Table 6. 1 Four basic indices

Index	Equation	Meaning
Index_{AP}	$\text{Index}_{APi} = \frac{\sum_{k=1}^{n} \left\lvert \frac{\partial \delta_k}{\partial P_i} \right\rvert}{npq}$	Active power to voltage angle
Index_{AQ}	$\text{Index}_{AQi} = \frac{\sum_{k=1}^{n} \left\lvert \frac{\partial \delta_k}{\partial Q_i} \right\rvert}{npq}$	Reactive power to voltage angle
Index_{VP}	$\text{Index}_{VPi} = \frac{\sum_{k=1}^{n} \left\lvert \frac{\partial \lvert V_k \rvert}{\partial P_i} \right\rvert}{npq}$	Active power to voltage magnitude
Index_{VQ}	$\text{Index}_{VQi} = \frac{\sum_{k=1}^{n} \left\lvert \frac{\partial \lvert V_k \rvert}{\partial Q_i} \right\rvert}{npq}$	Reactive power to voltage magnitude

The five compound indices are shown in Table 6. 2. Nodes with higher index value can be chosen as the location for storage placement for different concerns.

Table 6. 2 Five compound indices

Index	Equation	Meaning
Index_{P}	$\text{Index}_{AP} - \text{Index}_{VP}$	Active power to voltage angle, not voltage magnitude
Index_{Q}	$\text{Index}_{VQ} - \text{Index}_{AQ}$	Reactive power to voltage magnitude, not voltage angle
Index_{A}	$\text{Index}_{AP} - \text{Index}_{AQ}$	Active power to voltage angle, not reactive power
Index_{V}	$\text{Index}_{VQ} - \text{Index}_{VP}$	Reactive power to voltage magnitude, not active power
Index_{T}	$\text{Index}_{A} - \text{Index}_{V}$	Combine of active power to voltage angle and reactive power to magnitude

The indices are first tested on IEEE 14-node test feeder mainly because it has a simple configuration. The method is also applied to IEEE 123-node test feeder to show the indices work on the larger system as well. The indices proposed in this study can be used for selecting the optimal location for the storage system.

The suggested indices are validated by injecting active and reactive power on various nodes and observe the cumulative effect on the angle and magnitude. The trends have the same pattern as the sensitivity indices have predicted. The result shows that nodes with higher index value make more influence on voltage angle or magnitude.

The model of IEEE 123-node test feeder and IEEE 14-node test feeder are constructed with Matlab, cases are simulated by adding a storage device to PQ loads and moving the storage device all along PQ bus in the system to see the influence on the voltage angle and magnitude. The results suggested that the variations of voltage angle and magnitude are following the proposed indices.

The proposed indices can be used as a tool for planning the placement of storage system. Different indices can be chosen depending on the needed. In the proposed indices, Index_V or Index_Q can be used for selecting the best location of a capacitor bank since they only show the influence of injected reactive power over the voltage. Index_A or Index_P can be used to find the optimal place of a battery system. They only show the relation of the

active power on the angle. In general case of a storage device with an inverter that supposed to stabilize both of the angle and magnitude, Index_T is a suitable tool.

One of the advantages of the suggested method over the other iteration-based methods is that this approach does not require a loop and hence does not have convergence problems. The optimal location can be found straightforwardly.

6. 2 Future works

The test was successful as it was able to identify the node with the best performance on voltage angle and magnitude regulation. In this study, only the optimal location has been discussed. In future, the capacity of the energy storage device can also be optimized as well. Since the cost of a storage system depends on its size, it is important to find the optimal size for the storage system. The larger the storage system is, the more power can be injected into the system, but the cost would also increase. Optimal size and location of the storage device could make the system reach the best performance at the lowest cost.

REFERENCES

[1] F. Blaabjerg, Y. Yang, D. Yang and X. Wang, "Distributed Power-Generation Systems and Protection," in Proceedings of the IEEE, vol. 105, no. 7, pp. 1311-1331, July 2017.

[2] Y. Liu, J. R. Gracia, T. J. King and Y. Liu, "Frequency Regulation and Oscillation Damping Contributions of Variable-Speed Wind Generators in the U.S. Eastern Interconnection (EI)," in IEEE Transactions on Sustainable Energy, vol. 6, no. 3, pp. 951-958, July 2015.

[3] D. Cheng, B. A. Mather, R. Seguin, J. Hambrick and R. P. Broadwater, "Photovoltaic (PV) Impact Assessment for Very High Penetration Levels," in IEEE Journal of Photovoltaics, vol. 6, no. 1, pp. 295-300, Jan. 2016.

[4] P. Chiradeja and R. Ramakumar, "An approach to quantify the technical benefits of distributed generation," in IEEE Transactions on Energy Conversion, vol. 19, no. 4, pp. 764-773, Dec. 2004.

[5] A. Yadav and L. Srivastava, "Optimal placement of distributed generation: An overview and key issues," 2014 International Conference on Power Signals Control and Computations (EPSCICON), Thrissur, 2014, pp. 1-6.

[6] F. S. Abu-Mouti and M. E. El-Hawary, "Optimal DG placement for minimizing power loss in distribution feeder systems using sensory-deprived optimization algorithm," 2011 24th Canadian Conference on Electrical and Computer Engineering(CCECE), Niagara Falls, ON, 2011, pp. 000205-000209.

[7] M. Al-Muhaini and G. T. Heydt, "Evaluating Future Power Distribution System Reliability Including Distributed Generation," in IEEE Transactions on Power Delivery, vol. 28, no. 4, pp. 2264-2272, Oct. 2013.

[8] V. Kalkhambkar, R. Kumar and R. Bhakar, "Joint optimal allocation methodology for renewable distributed generation and energy storage for economic benefits," in IET Renewable Power Generation, vol. 10, no. 9, pp. 1422-1429, 10 2016.

[9] M. S. Lu, C. L. Chang, W. J. Lee and L. Wang, "Combining the Wind Power Generation System With Energy Storage Equipment," in IEEE Transactions on Industry Applications, vol. 45, no. 6, pp. 2109-2115, Nov.-dec. 2009.

[10] M. J. E. Alam, K. M. Muttaqi and D. Sutanto, "A Novel Approach for Ramp-Rate Control of Solar PV Using Energy Storage to Mitigate Output Fluctuations Caused by Cloud Passing," in IEEE Transactions on Energy Conversion, vol. 29, no. 2, pp. 507-518, June 2014.

[11] Q. Fu et al., "Generation capacity design for a microgrid for measurable power

quality indices," 2012 IEEE PES Innovative Smart Grid Technologies (ISGT), Washington, DC, 2012, pp. 1-6.

[12] S. G. Ghiocel and J. H. Chow, "A Power Flow Method Using a New Bus Type for Computing Steady-State Voltage Stability Margins," in IEEE Transactions on Power Systems, vol. 29, no. 2, pp. 958-965, March 2014.

[13] IEEE “IEEE PES Distribution System Analysis Subcommittee's Distribution Test Feeder Working Group,” August 2013. [Online]. Available: https://ewh.ieee.org/soc/pes/dsacom/testfeeders/

[14] M. J. Hossain, H. R. Pota, M. A. Mahmud and R. A. Ramos, "Investigation of the Impacts of Large-Scale Wind Power Penetration on the Angle and Voltage Stability of Power Systems," in IEEE Systems Journal, vol. 6, no. 1, pp. 76-84, March 2012.

[15] K. Kawabe and K. Tanaka, "Impact of dynamic behavior of photovoltaic power generation systems on short-term voltage stability," 2016 IEEE Power and Energy Society General Meeting (PESGM), Boston, MA, 2016, pp. 1-1.

[16] T. Moger and T. Dhadbanjan, "A novel index for identification of weak nodes for reactive compensation to improve voltage stability," in IET Generation, Transmission & Distribution, vol. 9, no. 14, pp. 1826-1834, 11 5 2015.

[17] R. S. Al Abri, E. F. El-Saadany and Y. M. Atwa, "Optimal Placement and Sizing Method to Improve the Voltage Stability Margin in a Distribution System Using Distributed Generation," in IEEE Transactions on Power Systems, vol. 28, no. 1, pp. 326-334, Feb. 2013.

[18] Z. Wu, D. W. Gao, H. Zhang, S. Yan and X. Wang, "Coordinated Control Strategy of Battery Energy Storage System and PMSG-WTG to Enhance System Frequency Regulation Capability," in IEEE Transactions on Sustainable Energy, vol. 8, no. 3, pp. 1330-1343, July 2017.

[19] J.J. Grainger, W.D. Stevenson, Power System Analysis (McGraw-Hill Inc., New York, St. Louis, San Francisco, Bogata, Caracas, Lisbon, London, Madrid, 1994)

[20] F. Tamp and P. Ciufo, "A Sensitivity Analysis Toolkit for the Simplification of MV Distribution Network Voltage Management," in IEEE Transactions on Smart Grid, vol. 5, no. 2, pp. 559-568, March 2014.

[21] R. Bottura, A. Borghetti, M. Barbiroli and C. A. Nucci, "Reactive power control of photovoltaic units over wireless cellular networks," 2015 IEEE Eindhoven PowerTech, Eindhoven, 2015, pp. 1-6.

[22] A. Yadav and L. Srivastava, "Optimal placement of distributed generation: An overview and key issues," 2014 International Conference on Power Signals Control and Computations (EPSCICON), Thrissur, 2014, pp. 1-6.

[23] H. Silva-Saravia, H. Pulgar-Painemal and J. M. Mauricio, "Flywheel Energy Storage

Model, Control and Location for Improving Stability: The Chilean Case," in IEEE Transactions on Power Systems, vol. 32, no. 4, pp. 3111-3119, July 2017.

[24] Y. M. Atwa and E. F. El-Saadany, "Optimal Allocation of ESS in Distribution Systems With a High Penetration of Wind Energy," in IEEE Transactions on Power Systems, vol. 25, no. 4, pp. 1815-1822, Nov. 2010.

[25] J. P. Barton and D. G. Infield, "Energy storage and its use with intermittent renewable energy," in IEEE Transactions on Energy Conversion, vol. 19, no. 2, pp. 441-448, June 2004.

[26] A. W. Bizuayehu, D. Z. Fitiwi and J. P. S. Catalão, "Advantages of optimal storage location and size on the economic dispatch in distribution systems," 2016 IEEE Power and Energy Society General Meeting (PESGM), Boston, MA, 2016, pp. 1-5.

[27] Y. Tang; S. H. Low, "Optimal Placement of Energy Storage in Distribution Networks," in IEEE Transactions on Smart Grid , vol.PP, no.99, pp.1-1

[28] Q. Sun, B. Huang, D. Li, D. Ma and Y. Zhang, "Optimal Placement of Energy Storage Devices in Microgrids via Structure Preserving Energy Function," in IEEE Transactions on Industrial Informatics, vol. 12, no. 3, pp. 1166-1179, June 2016.

[29] Y. Dvorkin, R. Fernández-Blanco, D. S. Kirschen, H. Pandžić, J. P. Watson and C. A. Silva-Monroy, "Ensuring Profitability of Energy Storage," in IEEE Transactions on Power Systems, vol. 32, no. 1, pp. 611-623, Jan. 2017.

[30] H. Pandžić, Y. Wang, T. Qiu, Y. Dvorkin and D. S. Kirschen, "Near-Optimal Method for Siting and Sizing of Distributed Storage in a Transmission Network," in IEEE Transactions on Power Systems, vol. 30, no. 5, pp. 2288-2300, Sept. 2015.

[31] C. Thrampoulidis, S. Bose and B. Hassibi, "Optimal Placement of Distributed Energy Storage in Power Networks," in IEEE Transactions on Automatic Control, vol. 61, no. 2, pp. 416-429, Feb. 2016.

[32] S. B. Karanki and D. Xu, "Optimal capacity and placement of battery energy storage systems for integrating renewable energy sources in distribution system," 2016 National Power Systems Conference (NPSC), Bhubaneswar, 2016, pp. 1-6.

[33] J. H. Teng, C. Y. Chen and I. C. Martinez, "Utilising energy storage systems to mitigate power system vulnerability," in IET Generation, Transmission & Distribution, vol. 7, no. 7, pp. 790-798, July 2013.

[34] M. Alonso and H. Amaris, "Voltage stability in distribution networks with DG," 2009 IEEE Bucharest PowerTech, Bucharest, 2009, pp. 1-6.

[35] Montoya Sanchez, Luis Fernando, "Novel Methodology to Determine the Optimal Energy Storage Location in a Microgrid to Support Power Stability" (2012). Theses and Dissertations. Paper 339.

[36] S. Wen, H. Lan, Q. Fu, D. C. Yu and L. Zhang, "Economic Allocation for Energy

Storage System Considering Wind Power Distribution," in IEEE Transactions on Power Systems, vol. 30, no. 2, pp. 644-652, March 2015.

[37] F. Mohammadi, H. Gholami, G. B. Gharehpetian and S. H. Hosseinian, "Allocation of Centralized Energy Storage System and Its Effect on Daily Grid Energy Generation Cost," in IEEE Transactions on Power Systems, vol. 32, no. 3, pp. 2406-2416, May 2017.